Geoscience Frontiers 10 (2019) 2045–2061

HOSTED BY

Contents lists available at ScienceDirect

China University of Geosciences (Beijing)

Geoscience Frontiers

journal homepage: www.elsevier.com/locate/gsf

Research Paper

Neoproterozoic tectonic geography of the south-east Congo Craton in Zambia as deduced from the age and composition of detrital zircons

Brandon L. Alessio [a,*], Alan S. Collins [a], Peter Siegfried [b], Stijn Glorie [a], Bert De Waele [c,d], Justin Payne [e], Donnelly B. Archibald [a,f]

[a] Centre for Tectonics, Resources and Exploration (TRaX), Dept of Earth Sciences, The University of Adelaide, Adelaide, South Australia 5005, Australia
[b] GeoAfrica Prospecting Services cc, Eros, Namibia
[c] SRK Consulting, 1/10 Richardson St, West Perth, Western Australia 6005, Australia
[d] Curtin University of Technology, Kent St, Bentley, Western Australia 6102, Australia
[e] Centre for Tectonics, Resources and Exploration (TRaX), School of Built and Natural Environments, University of South Australia, Adelaide, South Australia 5000, Australia
[f] St. Francis Xavier University, Physical Sciences Complex, 5009 Chapel Square, Antigonish, Nova Scotia B2G 2W5, Canada

ARTICLE INFO

Article history:
Received 29 September 2017
Received in revised form
8 May 2018
Accepted 22 July 2018
Available online 10 August 2018

Keywords:
Detrital zircon geochronology
Tectonics
Hafnium isotopes
Zambia
Southern irumide belt
Irumide belt

ABSTRACT

The Southern Irumide Belt (SIB) is an orogenic belt consisting of a number of lithologically varied Mesoproterozoic and Neoproterozoic terranes that were thrust upon each other. The belt lies along the southwest margin of the Archaean to Proterozoic Congo Craton, and bears a Neoproterozoic tectono-thermal overprint relating to the Neoproterozoic–Cambrian collision between the Congo and Kalahari cratons. It preserves a record of about 500 million years of plate interaction along this part of the Congo margin. Detrital zircon samples from the SIB were analysed for U–Pb and Lu–Hf isotopes, as well as trace element compositions. These data are used to constrain sediment-source relationships between SIB terranes and other Gondwanan terranes such as the local Congo Craton and Irumide belt and wider afield to Madagascar (Azania) and India. These correlations are then used to interpret the Mesoproterozoic to Neoproterozoic affinity of the rocks and evolution of the region. Detrital zircon samples from the Chewore–Rufunsa and Kacholola (previously referred to as Luangwa–Nyimba) terranes of the SIB yield zircon U–Pb age populations and evolved $\varepsilon_{Hf}(t)$ values that are similar to the Muva Supergroup found throughout eastern Zambia, primarily correlating with Ubendian–Usagaran (ca. 2.05–1.80 Ga) phase magmatism and a cryptic basement terrane that has been suggested to underlie the Bangweulu Block and Irumide Belt. These data suggest that the SIB was depositionally connected to the Congo Craton throughout the Mesoproterozoic. The more eastern Nyimba–Sinda terrane of the SIB (previously referred to as Petauke–Sinda terrane) records detrital zircon ages and $\varepsilon_{Hf}(t)$ values that correlate with ca. 1.1–1.0 Ga magmatism exposed elsewhere in the SIB and Irumide Belt. We ascribe this difference in age populations to the polyphase development of the province, where the sedimentary and volcanic rocks of the Nyimba–Sinda terrane accumulated in extensional basins that developed in the Neoproterozoic. Such deposition would have occurred following late-Mesoproterozoic magmatism that is widespread throughout both the Irumide and Southern Irumide Belts, presently considered to have occurred in response to collision between a possible microcontinental mass and the Irumide Belt. This interpretation implies a multi-staged evolution of the ocean south of the Congo Craton during the mid-Mesoproterozoic to late-Neoproterozoic, which ultimately closed during collision between the Congo and Kalahari cratons.

1. Introduction

The southern margin of the Palaeoproterozoic/Archaean Congo Craton is traced from the Namibian Central Damara Belt, to the Lufillian Arc and Zambezi Belt of Zambia, Zimbabwe, Malawi and

* Corresponding author.
E-mail address: brandon.alessio@adelaide.edu.au (B.L. Alessio).
Peer-review under responsibility of China University of Geosciences (Beijing).

https://doi.org/10.1016/j.gsf.2018.07.005

Mozambique (e.g. Collins and Pisarevsky, 2005; De Waele et al., 2008; Merdith et al., 2017). Collectively, these features are referred to the Damara–Lufilian–Zambezi orogen (Fig. 1). The orogen is of considerable significance as it contains the evidence of the tectonic geography of the Congo Craton through half a billion years of Earth history: from its role in Rodinia, including whether it was a part of Rodinia or not (Kröner and Cordani, 2003; De Waele et al., 2008), to its relationship with the Kalahari continent that is located to its present-day south. One curious feature of this orogen is that the geology of the central Damara region suggests relative tectonic quiescence during much of the Tonian period, with rifting occurring on the southern Congo Craton at ca. 760 Ma (McGee et al., 2012). In contrast, the Tonian was a time of volcanic arc magmatism and terrane accretion for the Zambezi Belt region and parts of Mozambique (Johnson et al., 2005; Bingen et al., 2009). Understanding this contrasting tectonic geography, apparently along orogenic strike, is required to understand the plate margin evolution of this region, a major step towards understanding the plate evolution record of Neoproterozoic central Gondwana (see Merdith et al., 2017).

The Southern Irumide Belt (SIB; Johnson et al., 2006) is a broadly ENE–WSW trending orogenic belt consisting of late Mesoproterozoic and Neoproterozoic metasedimentary and metaigneous rocks. The SIB is located between the Congo and Zimbabwe cratons (the northern part of the Neoproterozoic Kalahari Craton; Fig. 1) and has a Neoproterozoic structural overprint related to Gondwana amalgamation (Johnson et al., 2005; De Waele et al., 2008). In Zambia, the SIB has been the subject of relatively few studies leaving many questions unanswered regarding its origin and tectonic evolution. Late-Mesoproterozoic supra-subduction zone arc magmatism identified in the western-most Chewore–Rufunsa terrane, in conjunction with similar magmatism observed in Malawi and Mozambique (Bingen et al., 2009), implies the existence of an ocean to the south of the Congo Craton at this time

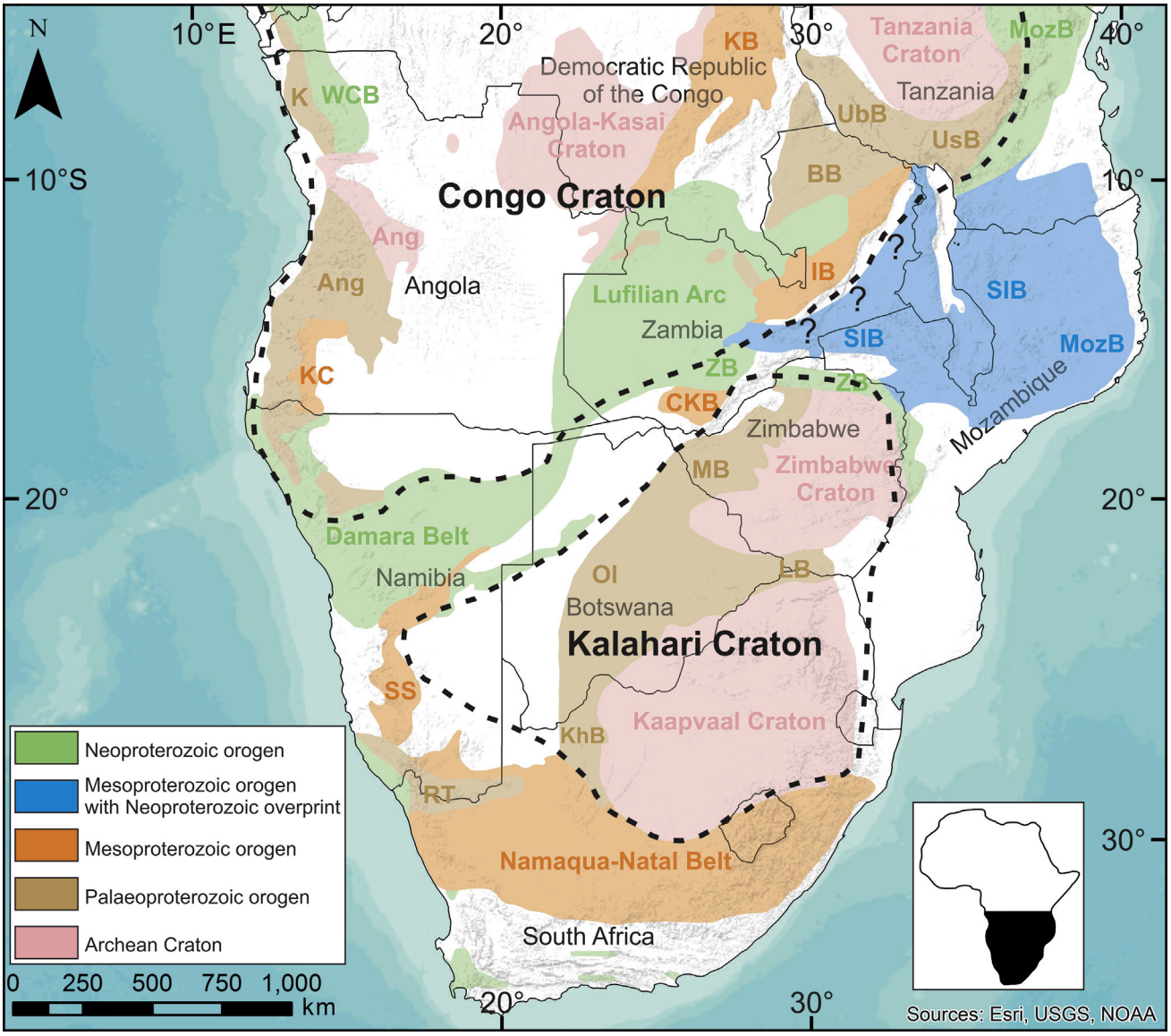

Figure 1. Simplified tectonic map of central Africa adapted from Hanson (2003) and Karmakar and Schenk (2016). The extent of the Congo and Kalahari cratons are denoted by the black dashed lines. Abbreviations: ANG, Angola Block; BB, Bangweulu Block; CKB, Choma-Kalomo Block; IB, Irumide Belt; K, Kimezian; KB, Kibaran Belt; KC, Kunene Complex; KhB, Kheis Belt; LB, Limpopo Belt; MB, Magondi Belt; MozB, Mozambique Belt; OI, Okwa Inlier; RT, Richtersveld Terrane; SIB, Southern Irumide Belt; UbB, Ubendian Belt; UsB, Usagaran Belt; WCB, West Congo Belt; ZB, Zambezi Belt.

(Johnson et al., 2007b; Begg et al., 2009). However, the evolution of such an ocean is poorly constrained at present. Furthermore, the southern and eastern margins of the Congo Craton were suggested as the source region for the abundant Palaeoproterozoic detrital zircons found in parts of central Madagascar and the Southern Granulite Terrane of India linking these regions to the Congo Craton in the Mesoproterozoic (Cox et al., 1998, 2004; Fitzsimons et al., 2004; Plavsa et al., 2014; Archibald et al., 2015). These relationships were the basis for proposing this region as a separate Neoproterozoic continent named Azania (Collins and Windley, 2002; Collins and Pisarevsky, 2005). However, the correlation was made based on the sparse data available at the time and has not been sufficiently tested, especially using other detrital fingerprints, such as zircon trace element and/or Lu–Hf isotopic compositions.

This study presents detrital zircon laser ablation inductively coupled plasma mass spectrometry (LA-ICP-MS) U–Pb isotope and trace element data in conjunction with multicollector LA-ICP-MS (LA-MC-ICP-MS) Lu–Hf isotope data from the SIB in Zambia. These data are used to constrain both the depositional ages of protoliths and isotopic nature of zircon sources for metasedimentary lithologies found within the three western-most terranes (Chewore–Rufunsa, Kacholola, and Nyimba–Sinda) of the SIB. These data are compared to neighbouring terranes to suggest correlations between major metasedimentary sequences in the SIB, elsewhere in Africa and even further afield in Madagascar and India. These correlations can represent depositional connections, where both basins received input for the same sources, providing palaeogeographic constraints for the southern Congo margin.

2. Regional geology

2.1. The eastern Congo Craton

The Congo Craton refers to the amalgamated central African landmass at the time of Gondwana assembly (De Waele et al., 2008), and is comprised of several cratonic blocks. The Bangweulu Block and Tanzanian Craton are located to the eastern side of the Congo Craton (Fig. 1) and are interpreted to have a formed a single continental block from the early Proterozoic onwards, suggested to be marked by the Ubendian–Usagaran orogen. This ca. 2.05–1.80 Ga orogen is interpreted to have been a long lived active margin that is now located between the two cratons, along the southern margin of the Tanzanian Craton. The Bangweulu Block lies south of the Tanzanian Craton, in northern Zambia. This block is characterised by basement lithologies consisting of schists and coarse to porphyritic granitoids, which are unconformably overlain by fluvial, aeolian and lacustrine sediments of the Paleoproterozoic Muva Supergroup (Daly and Unrug, 1982; De Waele et al., 2006a). De Waele et al. (2006b) suggested that the nucleus of the Bangweulu Block is an Archean craton but contact relationships are obscured by these Palaeoproterozoic sediments. Granitoids in the Bangweulu Block that formed at ca. 1.85 Ga, are undeformed and have high-K, calc-alkaline geochemical characteristics (Brewer et al., 1979; Schandelmeier, 1980, 1983; De Waele et al., 2006b). These were interpreted by Brewer et al. (1979) as shallow intrusions as they are associated with volcanism, which were suggested to represent an active volcanic arc (Daly and Unrug, 1982). De Waele et al. (2006b) noted a lack of evidence for crustal thickening and exhumation in the Bangweulu Block that would be associated with such an arc. De Waele et al. (2006b) additionally noted that the E–W trending schist belts of the Bangweulu Block appear to merge with similar lithologies of the NNW–SSE trending Ubendian Belt at some localities, but are terminated by shear zones in others.

2.2. The Irumide Belt

The Irumide Belt *sensu stricto* (herein referred to as the Irumide Belt) is located to the south of the Bangweulu Block (Fig. 1) and is a NE–SW trending Mesoproterozoic orogenic belt comprised of deformed Palaeoproterozoic granitic basement, folded metasedimentary units and voluminous granitoid intrusions of ca. 1.05–1.00 Ga age (Daly, 1986; De Waele et al., 2006a, 2009). The metasedimentary units consist of a succession of quartzites and metapelites and are grouped into the Muva Supergroup, which is interpreted to have been deposited during the Palaeoproterozoic. SHRIMP U–Pb detrital zircon ages from the Muva Supergroup are in the range of ca. 3.2–1.8 Ga with major peaks at ca. 2.1 Ga and 1.9 Ga. The maximum depositional age is ca. 1.85 Ga with a minimum depositional age of ca. 1.6 Ga constrained by granite emplacement in the Irumide Belt (De Waele et al., 2003; De Waele and Fitzsimons, 2007). Peak metamorphism in the Irumide Belt is interpreted to have occurred at ca. 1020 Ma and is represented by upper-amphibolite facies (7–8 kbar and ~650 °C) mineral assemblages (De Waele, 2004). Peak metamorphism is coincident with large scale structural overprinting along the southern margin of the belt and by the intrusion of primarily calc-alkaline granitoids. The lack of juvenile material present in the Irumide Belt has been used to suggest that the belt acted as a passive margin on the southeast margin of the Congo Craton, and that the active continental margin was further south and is represented by the SIB (De Waele et al., 2006b).

2.3. The Southern Irumide Belt

2.3.1. Regional context, extent and correlations

Early work noted deformed Mesoproterozoic rock south of the Irumide Belt, which had been considered as part of the Mozambique Belt and/or Irumide Belt (Johns et al., 1989). The term Southern Irumide Belt was later introduced by Johnson et al. (2005), who consider the belt to be distinct (detailed below) and separate to the Irumide and Mozambique belts. The Southern Irumide Belt remains the focus of ongoing research due to the suggestion that it represents a discrete continental block that was accreted to the Congo crustal assemblage (De Waele et al., 2006b, 2008; Johnson et al., 2007b; Begg et al., 2009). Lithologies of the SIB crop out in Zambia, Malawi, Mozambique, and Tanzania (Fig. 1). In Zambia, the SIB is located immediately south of the Irumide Belt though any continuity/discontinuity between the SIB and Irumide Belt is obscured by a Permo–Triassic Karoo Graben that forms the Luangwa Valley (Johnson et al., 2006). Aeromagnetic data have been used to interpret that a major shear zone (Mwembeshi Shear Zone) runs between the belts, though this feature is concealed by the graben sediments (Johnson et al., 2006; Sarafian et al., 2018). The Zambian portion of the SIB has been subdivided into four imbricated terranes, from west to east these terranes have been referred to as the Chewore–Rufunsa, Luangwa–Nyimba, Petauke–Sinda, and Chipata terranes (Fig. 2; Mapani et al., 2004; Johnson et al., 2006). Here we partially adopt the nomenclature of these studies, though we instead refer to the Luangwa–Nyimba Terrane as the Kacholola Terrane. This name instead refers to a location within the terrane, as the towns of Luangwa and Nyimba are either on the shear zone boundary or outside the defined area of the terrane. We also refer to the Petauke–Sinda Terrane instead as the Nyinba–Sinda Terrane, which better encompasses the extent of fault-bounded Neoproterozoic lithologies comprising this terrane. In the Tete Province of northwest Mozambique, the SIB has been subdivided into a series of terranes with supracrustal sequences that display little cohesion and granitoids with ages ranging from ca. 1.2 Ga to 1.05 Ga (Westerhof et al., 2008). The sediments in these terranes display detrital zircon age populations of ca. 2.7, 2.5, 2.1,

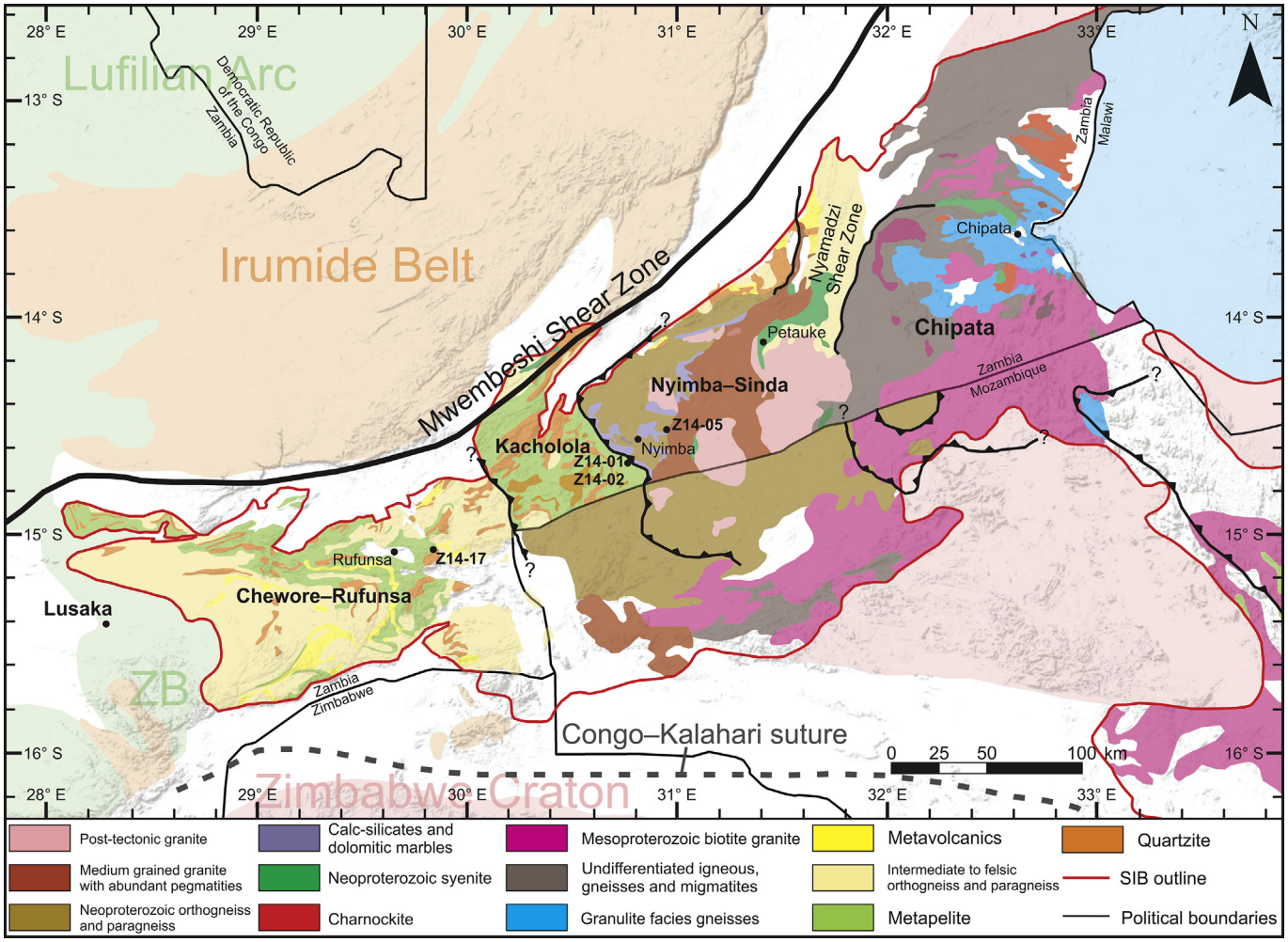

Figure 2. Simplified tectonic map of eastern Zambia adapted from Johnson et al. (2006), with geological units distinguished for the SIB in Zambia and Mozambique. Lithological data for Zambia is adapted from the Geological Survey of Zambia (Agar, 1984; Ray, 1984; Vayrda, 1984) and Johnson et al. (2006). Lithological data for Mozambique is adapted from Westerhof et al. (2008). Shading for Malawi and tectonic units outside of the SIB and Malawi follow the legend in Fig. 1.

1.9, 1.3 and 1.2 Ga (Westerhof et al., 2008, and references therein). In northeast Mozambique a number of Palaeoproterozoic to Mesoproterozoic complexes that record variable degrees of late-Neoproterozoic metamorphism have been identified (Bingen et al., 2009; Boyd et al., 2010). The Mesoproterozoic Unango and Marrupa complexes identified in this region primarily consist of ca. 1.1 to 1 Ga orthogneiss, and are interpreted to have formed on the Congo margin with the SIB, possibly representing an eastern continuation of the belt. Neoproterozoic granitoids in southern Tanzania have been linked with these rocks in Mozambique, and possibly represent a continuation of the Marrupa Complex (Hauzenberger et al., 2014; Thomas et al., 2014). Later work identified rocks bearing ca. 1.0 Ga overprints in southern Tanzania, additionally observing an orthogneiss that yields a crystallisation age of ca. 1.1 Ga. This work also analysed a sample of quartzite in a metasedimentary sequence with marble, which was shown to contain predominantly ca. 1.1–1.0 Ga detritus with ca. 2.7 Ga and 2.0 Ga populations. This is suggested to represent a post-Irumide basinal sequence, with no rigorous constraint on a minimum depositional age (Hauzenberger et al., 2014; Thomas et al., 2016). Similar rocks are also preserved in the Nampula Complex of northeast Mozambique, which is also comprised of ca. 1.1–1.0 Ga orthogneiss that is generally older than that preserved in the Unango and Marrupa complexes. However, this complex is instead interpreted to have accreted to the Kalahari Craton prior to Congo–Kalahari collision (Macey et al., 2010). This collision resulted in its current position, separated from the other Mesoproterozoic complexes by the WSW–ENE trending Lurio Belt that is suggested to represent a suture zone between the Congo and Kalahari cratons (Bingen et al., 2009).

2.3.2. Timing of magmatism and metamorphism in the SIB

SIB magmatism is constrained to between ca. 1095 and 1040 Ma in Zambia and northwest Mozambique (Fig. 3; Johnson et al., 2006, 2007b; Westerhof et al., 2008) and involved the contamination of juvenile material by silicic continental crust, typical of a continental-margin-arc setting (Johnson et al., 2007b). Here, metamorphism is identified as high-temperature, low-pressure and is contemporaneous with magmatism. The tectonic settings of the eastern terranes in this area are poorly constrained, though preliminary work suggests these to be components of an accreted island arc complex or a continuation of the continental-margin-arc (Mapani et al., 2001; Johnson et al., 2006, 2007b). In northeast Mozambique, SIB magmatism is constrained to between ca. 1060 Ma and 950 Ma (Fig. 3; Bingen et al., 2009). The magmatism in these Mesoproterozoic complexes is both voluminous and felsic in composition, and as such is also interpreted to have formed in a continental-margin-arc setting. Notably, metamorphism in the

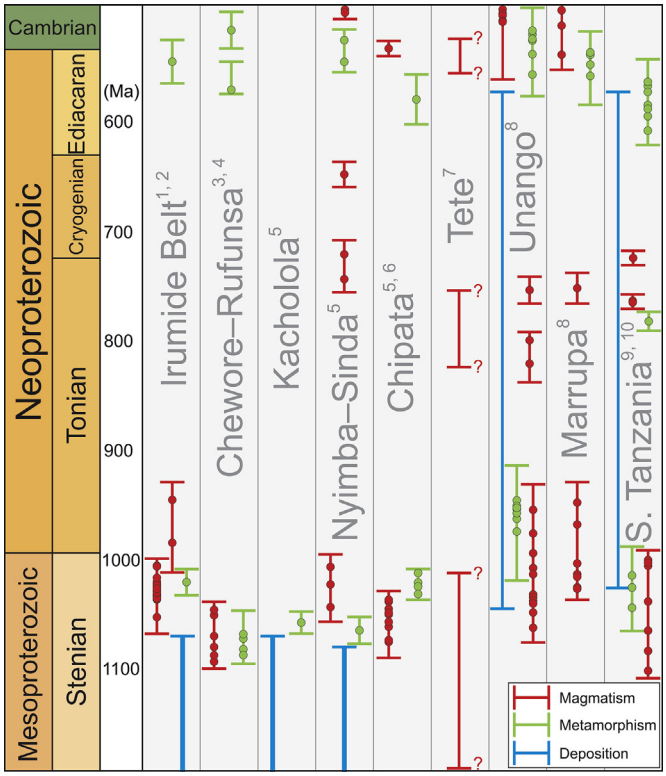

Figure 3. Time-space plot of existing data for the SIB, indicating periods of magmatism (red), metamorphism (green), and deposition (blue) for the belt throughout the Stenian to middle Cambrian. Bars throughout the plot indicate the duration of events defined by the maximum and minimum error ranges of a series of analyses. Circles along plotted bars indicate mean age values obtained via U–Pb geochronology. References are indicated by the numbers accompanying a given unit's name and are as follows: 1, De Waele et al. (2006a); 2, De Waele et al. (2009); 3, Johnson et al. (2007b); 4, Goscombe et al. (2000); 5, Johnson et al. (2006); 6, Karmakar and Schenk (2016); 7, Westerhof et al. (2008; approximate age ranges); 8, Bingen et al. (2009); 9, Hauzenberger et al. (2014); 10, Thomas et al. (2016).

Unango and Marrupa complexes is younger than that recorded in Zambia and northwest Mozambique, instead dated at ca. 950 Ma. U–Pb, Hf and Nd isotopic data obtained by Johnson et al. (2007b) suggest that the Zambian terranes of the SIB were formed on variably reworked Palaeoproterozoic basement. Similarly, Archaean to Palaeoproterozoic components are also identified in northeast Mozambique (Bingen et al., 2009). A marginal basin ophiolite (Chewore ophiolite) dated at 1393 ± 22 Ma (Oliver et al., 1998) was observed in northern Zimbabwe, though lithological and geochemical characteristics suggest that it is not directly related to the ca. 1070 Ma continental-margin-arc magmatism (De Waele et al., 2008; Westerhof et al., 2008). Younger magmatic rocks in the belt are broadly restricted to the Nyimba–Sinda Terrane in Zambia as well as the Unango and Marrupa complexes of Mozambique (Fig. 3). A syenite pluton in the Unango Complex yields a crystallisation age of 799 ± 8 Ma, while a charnockite pluton in the Marrupa Complex yielded a crystallisation age of 753 ± 13 Ma and metamorphic age of 549 ± 22 Ma (Bingen et al., 2009). The ages yielded by this pluton are both within error of similar ages recorded by widespread orthogneiss located within the Nyimba–Sinda Terrane, which yields protolith U–Pb ages of 742 ± 13 Ma and has an interpreted metamorphic age of 536 ± 10 Ma (Johnson et al., 2006). This gneiss is interpreted to be closely associated with predominantly andesitic volcanics that are also located in this terrane (Barr and Drysdall, 1972; Johnson et al., 2006). Direct age constraints are not available for the volcanics, though underlying granite has yielded a crystallisation age of ca. 1040 Ma. Post-kinematic granite is also widespread throughout the Nyimba–Sinda Terrane and yields a crystallisation age of ca. 500 Ma. This is broadly consistent with the syenite intrusions found within the prominent Nyamadzi Shear Zone north-east of the Nyimba–Sinda Terrane (Johnson et al., 2006). Broadly coeval post-kinematic magmatism is observed in the complexes of northeast Mozambique, with crystallisation ages ranging from ca. 550 Ma to 490 Ma (Fig. 3; Bingen et al., 2009).

2.3.3. Relationship to the Irumide Belt and Congo Craton

Several distinct differences can be observed between the SIB and the Irumide Belt, which has led a number of authors to conclude that there is no genetic relationship between the two belts (Johnson et al., 2006, 2007b; De Waele et al., 2008; Westerhof et al., 2008; Hauzenberger et al., 2014). While the SIB contains an array of deformed sedimentary, igneous and volcanic units with related intrusions (Johnson et al., 2006, 2007b; De Waele et al., 2006b; Westerhof et al., 2008; Hauzenberger et al., 2014), the Irumide Belt is largely composed of granitoids and the metasedimentary Muva Supergroup (Daly and Unrug, 1982; Daly et al., 1984; Daly, 1986; De Waele and Mapani, 2002). Metamorphism in the Irumide Belt occurred at ca. 1020 Ma and involved pressures around 7–8 kbar as a result of crustal thickening processes. This is distinct from metamorphism in the SIB, which was considered to have occurred between ca. 1090 and 1040 Ma and involved peak pressures below 4 kbar (Goscombe et al., 2000; Johnson et al., 2006, 2007b). Johnson et al. (2007b) argued that this difference in the timing and nature of metamorphism without a gradual transition is unlikely to be due to the diachronous development of a single Irumide belt. However, recent pressure–temperature estimates obtained for the Chipata Terrane by Karmakar and Schenk (2016) yield values of ~900–1000 °C and 5–6 kbar. These authors also obtained U–Pb monazite ages that indicate that metamorphism was contemporaneous with that in the Irumide Belt. On the basis of contrasting styles and timing of metamorphism, as well as the Mwembeshi dislocation between the SIB and Irumide Belt, Johnson et al. (2006) suggested that there is no genetic relationship between the belts and that the presence of the Luangwa Valley between them masks a key suture along the margin of the Congo Craton. With no genetic relationship between the belts, Johnson et al. (2007b) argued that the SIB did not develop on the Congo margin and instead developed via subduction of continental crust under the margin of a micro-continental mass later named the Rushinga Microcontinent (Begg et al., 2009), which ultimately lead to ocean closure at ca. 1040 Ma. This model suggests that collision between the SIB and Congo craton margin led to the cessation of magmatism in the SIB, and initiated compression and crustal melting in the Irumide Belt. Alternatively, Bingen et al. (2009) suggested that the terranes and complexes identified in the SIB could have always been a part of the southern Congo margin, which acted a long-lived active margin and experienced at least one event of foreland propagation between ca. 1020 Ma and 1005 Ma.

3. Methods

Three samples of quartzite (Z14-01, Z14-02, Z14-17) and one sample of psammite (Z14-05) were collected for detrital zircon U–Pb geochronology, trace element analysis and Lu–Hf isotopic analysis from the SIB in Zambia. Three additional detrital zircon samples from the Irumide Belt were analysed for Lu–Hf isotopic data. These samples were previously age dated using U–Pb geochronology, the details of which are reported in De Waele et al. (2006a).

3.1. U–Pb detrital zircon geochronology

U–Pb and trace element data were obtained from separated detrital zircon grains that were extracted from crushed rocks using standard magnetic and heavy liquid techniques. Zircon separates were hand-picked, mounted in epoxy resin and then polished to expose the grains. The grains were imaged using an FEI Quanta 600 Scanning Electron Microscope (SEM) with a Gatan cathodoluminescence detector attached to identify compositional domains that were suitable for analysis. Zircon grains were analysed for U–Pb isotopes and trace elements using an Agilent 7900 ICP-MS and NewWave UP213 Laser Ablation System. Trace elements analysed include the rare earth elements (REE; with the exception of Pm) and P. Ablation of zircon was performed in a He-atmosphere with a frequency of 5 Hz. A spot size of 30 μm was used for all analyses. A total acquisition time of 60 s was used consisting of 30 s of background acquisition followed by 30 s of sample ablation. The standard GJ ($^{206}Pb/^{238}U = 608.5 \pm 0.4$ Ma; Jackson et al., 2004) was used as the primary standard for all zircon analyses and Plešovice ($^{206}Pb/^{238}U = 337.13 \pm 0.37$ Ma; Sláma et al., 2008) was used as a secondary standard. Standard glass NIST SRM 610 was used during trace element analysis as a reference material for corrections to mass bias drift. Plešovice yielded a 95% concordant average $^{206}Pb/^{238}U$ age of 332.1 ± 2.4 Ma (2σ, $n = 61$) and $^{207}Pb/^{206}Pb$ age of 333.7 ± 9.9 Ma (2σ, $n = 61$). U–Pb data were reduced using *GLITTER* (Jackson et al., 2004), while trace element data were reduced using *IOLITE* (Paton et al., 2011). Upper and lower concordia intercepts of samples were calculated using *ISOPLOT* (Ludwig, 2004), in addition to the modelling method of Reimink et al. (2016).

3.2. Lu–Hf isotope analysis

Lu–Hf isotope analysis in zircon was conducted at the University of Adelaide using a New Wave UP-193 Excimer laser attached to a Thermo-Scientific Neptune Multi-Collector ICP-MS. Analytical methods follow Payne et al. (2013). A spot size of ~50 μm was used for all appropriately sized zircon grains, decreasing to 35 μm for smaller grains. Zircons were ablated in a He atmosphere, which was mixed with Ar upstream of the ablation cell, for between 40 s and 100 s with a 5 Hz repetition rate, a 4 ns pulse rate, and an intensity of ~6–8 J/cm^2. Data were normalised to $^{179}Hf/^{177}Hf = 0.7325$, using an exponential correction for mass bias. Yb and Lu isobaric interferences on ^{176}Hf were corrected for following the methodology of Woodhead et al. (2004). Reduction of zircon data was undertaken using the Hf isotope data reduction spreadsheet, *HfTRAX* (Payne et al., 2013). Known reference materials (Mud Tank and Plešovice) were run throughout the analytical session to verify the stability and performance of the instrument. The primary standard used was Plešovice, which yielded a mean $^{176}Hf/^{177}Hf$ ratio of 0.282470 ± 0.000015 (2σ, $n = 7$). This is within uncertainty of the known value of 0.282482 ± 0.000013 (Sláma et al., 2008).

4. Sample information and analytical results

4.1. Southern Irumide Belt samples

4.1.1. Z14-17 (15°03′09.6″S, 29°50′59.8″E)

Z14-17 is a pure quartzite collected from the Chewore–Rufunsa Terrane (Fig. 2), in a road cutting along Great East Road, approximately 20 km northeast of Rufunsa. Zircon grains from this sample range from ~50 μm to 200 μm in length, and vary from stubby (1:1) or elongated (4:1). They range in appearance from clear to dark and cloudy. Some grains display oscillatory zonation that reflect the igneous growth of the grains and all grains display rounding typical of detrital zircons (Fig. 4). In many cases, the CL zoning indicates that the rims of zircon grains were destroyed, possibly as a result of sedimentary abrasion, metamorphism or chemical alteration (Corfu et al., 2003). Some zircon grains appear to be fragments of a larger grain. One hundred and seventeen (117) zircon cores and six rims were randomly selected for U–Pb LA-ICP-MS analysis, of which 62 cores were ≤10% discordant (Fig. 5a). The $^{207}Pb/^{206}Pb$ ages of these near-concordant analyses range from ca. 2726 Ma to 1768 Ma, with the majority of analyses yielding ages around 2.0 Ga. The Kernel Density Plot (KDP) for this sample (Fig. 5b) displays a prominent peak at ca. 2.0 Ga, with smaller peaks at ca. 1.8, 2.2, 2.6, 2.7, and 3.2 Ga. Hafnium data was obtained for 15 zircon grains from the ca. 1.8, 2.0, 2.6 and 3.2 Ga populations (Fig. 6). Each population has negative $\varepsilon_{Hf}(t)$ values, ranging from −5.9 to −0.3. A single grain with a ca. 2.5 Ga age has an $\varepsilon_{Hf}(t)$ value of +5.2. Trace element data were obtained for the same 15 zircons (Fig. 7a), which display REE concentrations typical of zircon (Hoskin and Ireland, 2000) that shows a general increase in elemental abundance with increasing atomic mass. Such a trend is also observed in each subsequent sample. Phosphorous contents range of ~100–900 ppm (Fig. 7d), with zircons between ca. 2.0 and 1.8 Ga having generally higher P contents than older grains. U, Yb and Hf values obtained from all analyses (in every sample) are consistent with zircon derived from a continental source (Fig. 7e and f; Grimes et al., 2007).

4.1.2. Z14-01 (14°38′02.3″S, 30°47′36.7″E) and Z14-02 (14°38′04.5″S, 30°47′52.3″E)

Z14-01 was collected from the base of Lupiri Hill in the Kacholola Terrane, approximately 9 km SW of Nyimba. Z14-02 was collected from the top of Lupiri Hill (Fig. 2). Both samples are quartzite and contain minor muscovite. Zircons from these samples are ~40 μm to 200 μm in length, ranging from stubby (1:1) or elongated (4:1). Zircon grains from Z14-01 are generally clear to dark in appearance, with some brownish grains present. Zircon grains from Z14-02 are clear in appearance. Grains in both samples commonly display oscillatory zonation that reflect the igneous growth of the grains, while all grains display rounding (Fig. 4). In sample Z14-01, 136 zircon cores and four rims were randomly selected for U–Pb analysis, from this population 84 grain cores were ≤10% discordant. 23 zircon core analyses and five rim analyses were obtained from sample Z14-02 and seven cores were ≤10% discordant. Due to the proximity, common zircon morphology and similarity in ages obtained, in conjunction with the paucity of near concordant analyses from Z14-02, the analyses from these samples have been combined and are displayed on a Wetherill concordia diagram (Fig. 5c). The $^{207}Pb/^{206}Pb$ ages of these near-concordant analyses range from ca. 3376 Ma to 1764 Ma and most ages are ca. 2.0 Ga. The KDP for this sample (Fig. 5d) displays a large age peak at ca. 2.0 Ga, with smaller peaks at ca. 1.85, 2.3, 2.7 and 3.4 Ga. Hafnium isotopic data were obtained for 22 zircons from each of the populations. Each age population has negative $\varepsilon_{Hf}(t)$ values (Fig. 6) that range from −19.8 to −0.1. A single grain with a ca. 3.3 Ga age displays an $\varepsilon_{Hf}(t)$ value of +7.8. P concentrations in these samples vary between ~100–800 ppm, with a higher variation in P content in zircons of ca. 2.0–1.8 Ga age in comparison to older grains.

4.1.3. Z14-05 (14°31′58.9″S, 30°57′50.0″E)

Z14-05 was collected in the Nyimba–Sinda Terrane, from an outcrop approximately 15 km east of Nyimba, along the Great East Road (Fig. 2). The sample is a psammite, being less pure than the previous quartzite samples and containing approximately 10% microcline and minor plagioclase. It also contains minor chlorite, muscovite and rutile. Zircons are between ~20 μm and 120 μm in

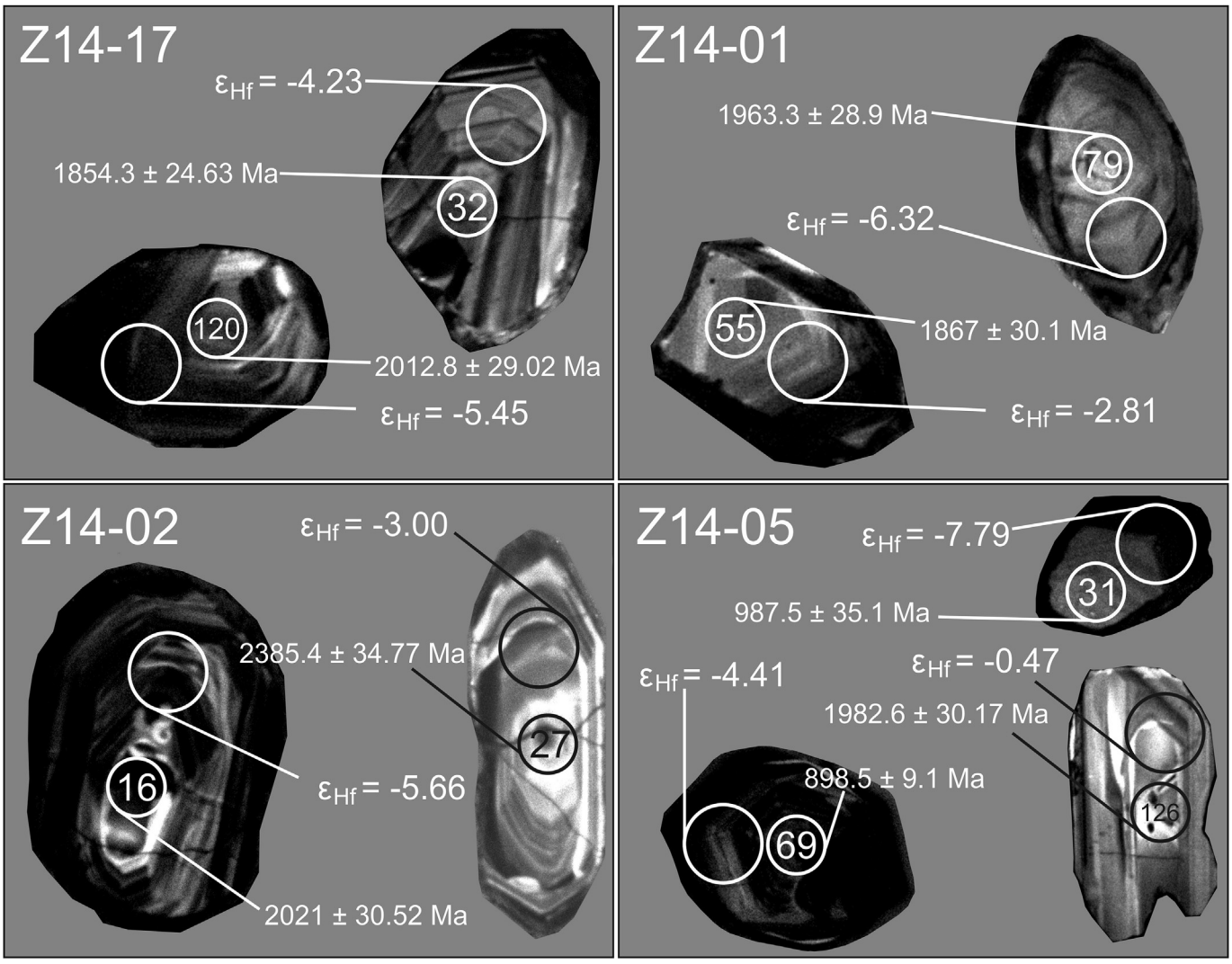

Figure 4. Cathodoluminescence (CL) images of zircons from samples selected for geochronological analysis. Numbered circles represent LA-ICP-MS spot locations of 30 μm diameter and the larger circles on each grain represent MC-LA-ICP-MS spot locations.

length and are stubby (1:1) to elongated (4:1) and are clear in appearance. The zircons typically display oscillatory zonation and all grains are rounded (Fig. 4). Some grains display deformed or discontinuous zonation at the rims, which may reflect partially metamorphosed grains or a later stage of growth. The fractured appearance and zonation of some grains indicates that the grains are fragments of a larger grain. One hundred and twenty two zircon cores and nine rims were randomly selected for U–Pb analysis (Fig. 5e) and 52 core analyses are ≤10% discordant. The $^{206}Pb/^{238}U$ and $^{207}Pb/^{206}Pb$ ages are between ca. 653 Ma and 2058 Ma, with the majority of analyses clustering at ca. 1.0 Ga. For grains >1.2 Ga, the $^{207}Pb/^{206}Pb$ age has been considered, while the $^{206}Pb/^{238}U$ age has been used for younger grains. The KDP for this sample (Fig. 5f) displays a prominent age peak at ca. 1.0 Ga, with minor populations at ca. 0.7 Ga and 2.0 Ga. The enlarged section of the concordia diagram for this sample (Fig. 5e), shows several discordant analyses on a near-linear trajectory between the concordant ca. 1.0 Ga analyses and ca. 700–600 Ma analyses. This may suggest that these younger concordant analyses are part of the ca. 1.0 Ga population but experienced subsequent Pb loss.

Concordance plotted against the $^{206}Pb/^{238}U$ age (Fig. 8a) for each zircon display a strong linear trend between ca. 1100 Ma and 760 Ma. This implies that the discordant analyses within this age range that were pulled along a Discordia from ca. 1100 Ma and may have formed a coherent single population at that age prior to Pb-loss. The deviation of the <760 Ma ages from the $^{206}Pb/^{238}U$-concordance trendline means that it is not possible to unambiguously assign them to the same population using this method. It does not exclude them from this initial population though as the potential exists for ancient lead loss of a different age to have resulted in a different relationship between $^{206}Pb/^{238}U$ ages and concordance. Assessing the $^{232}Th/^{238}U$ ratios against $^{206}Pb/^{238}U$ ages for the same analyses (Fig. 8b) shows a relatively consistent trend of decreasing $^{232}Th/^{238}U$ with decreasing age, which has been linked to Pb loss (Pidgeon, 1992; Pidgeon et al., 1998; Ashwal et al., 1999; Vavra et al., 1999; Hoskin and Black, 2000; Collins, 2003; Collins et al., 2004; Kirkland et al., 2015). Hf isotope analyses of < ca. 1000 Ma grains show similar Hf_i values to grains from the ca. 1.0 Ga population (Fig. 8c). The upper and lower concordia intercepts of this population are identifiable using the modelling method of Reimink et al. (2016). This method produces a series of discordia lines and calculates an associated summed probability density, which serves as a measure of the likelihood that a given line contains discordant analyses. Likelihood in this context serves as a relative metric for deciphering upper and lower intercept

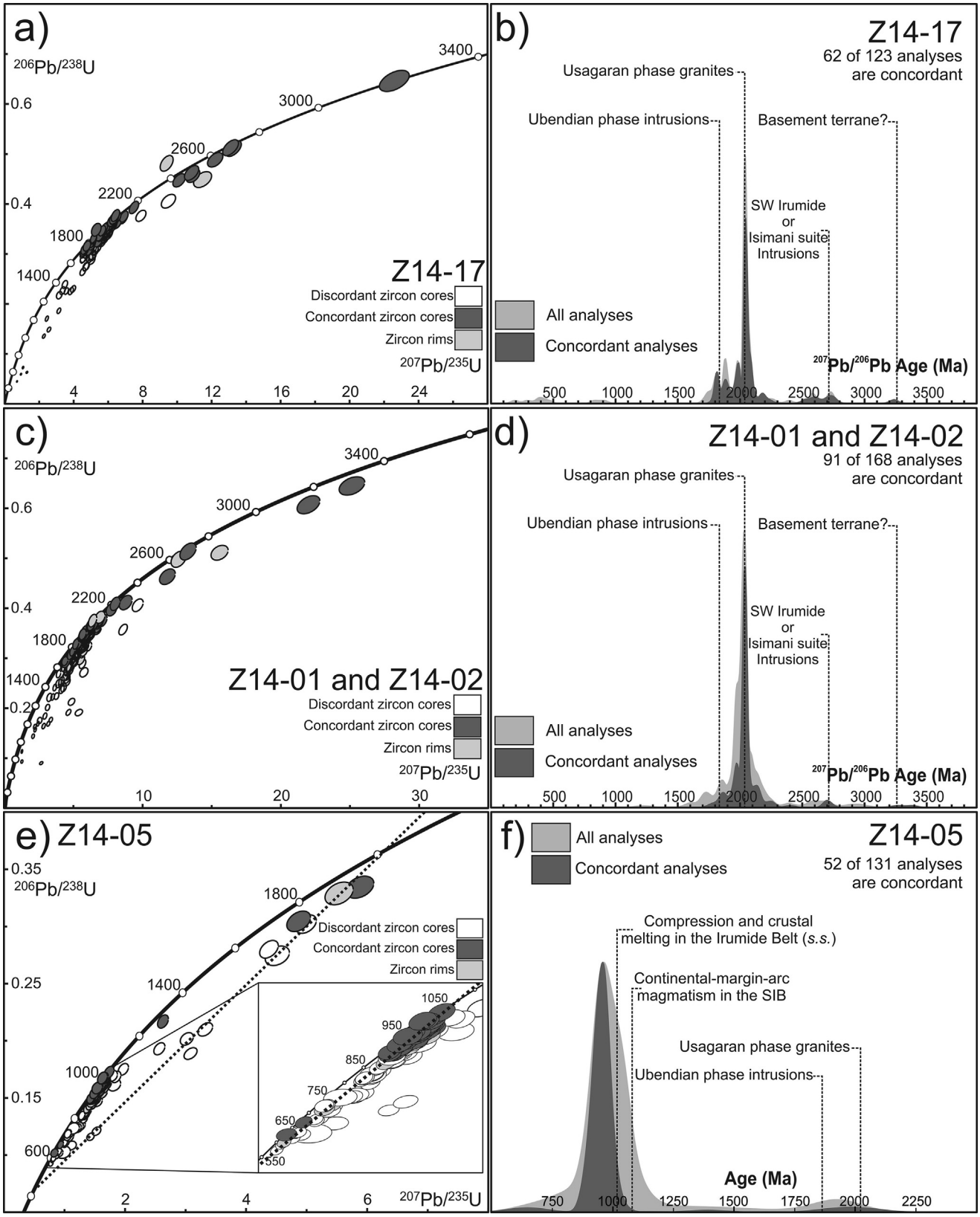

Figure 5. U–Pb concordia diagrams and associated Kernel Density Plots (KDPs) for samples from the Southern Irumide Belt. (a) Concordia diagram for sample Z14-17 of the Chewore–Rufunsa Terrane, ≥ 90% concordant zircons are shaded in dark grey and rims in light grey. (b) Associated KDP for Z14-17 with $^{207}Pb/^{206}Pb$ ages plotted, likely sources are indicated by the dashed lines. (c) Concordia diagram for samples Z14-01 and Z14-02 of the Kacholola Terrane, ≥ 90% concordant zircons are shaded in dark grey and rims in light grey. (d) Associated KDP for Z14-01 and Z14-02 with $^{207}Pb/^{206}Pb$ ages plotted, likely sources are indicated by the dashed lines. (e) Concordia diagram for sample Z14-05 of the Nyimba–Sinda Terrane, a blowout is also depicted for the ca. 1.1–0.55 Ga age range. ≥ 90% concordant zircons are shaded in dark grey and rims in light grey. Interpreted Pb loss lines are indicated by the dashed lines in the concordia plot and blow out. (f) Associated KDP for Z14-05 with $^{206}Pb/^{238}U$ ages plotted for ages < 1.2 Ga and $^{207}Pb/^{206}Pb$ ages plotted for ages > 1.2 Ga. Likely sources are indicated by the dashed lines.

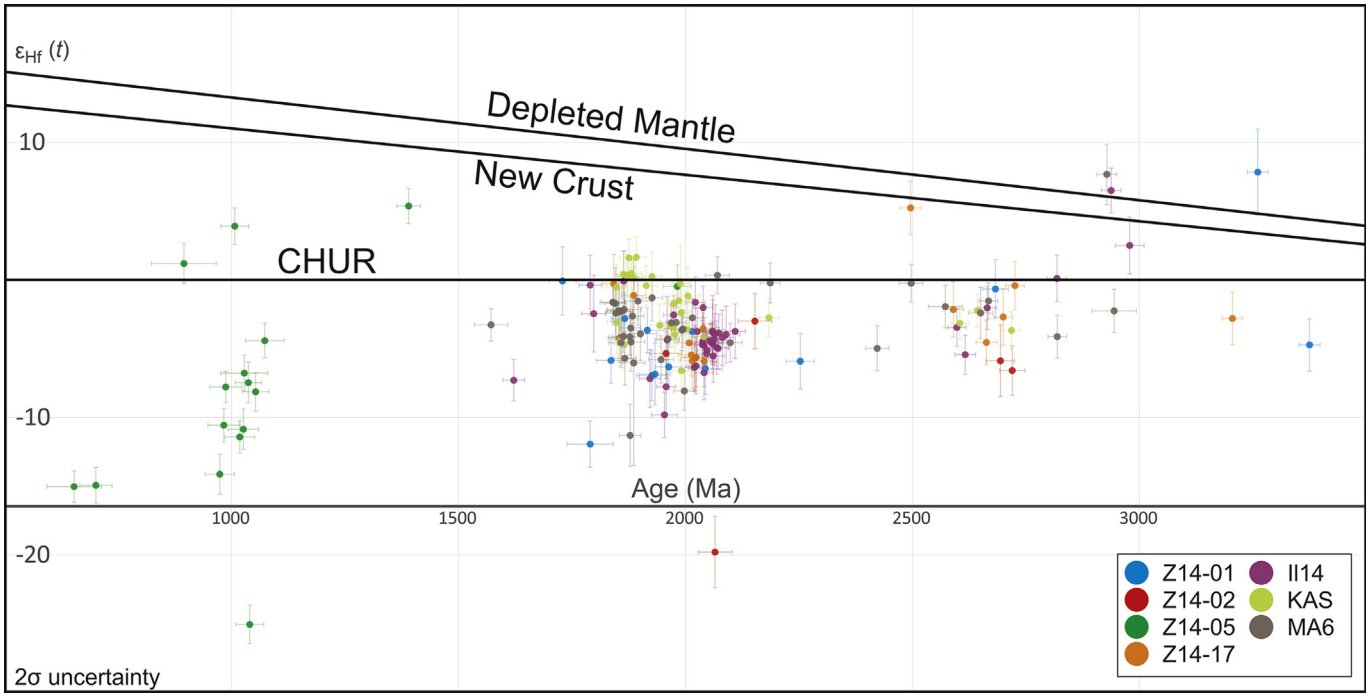

Figure 6. $\varepsilon_{Hf}(t)$ versus U–Pb age plot for detrital zircons from the Irumide Belt and SIB. Uncertainty for age and $\varepsilon_{Hf}(t)$ values are shown at the 2σ level. The depleted mantle curve of Griffin et al. (2002) is plotted, as is the new crust line of Dhuime et al. (2011).

ages. Fig. 8d is a visualisation of these chords and their relative likelihoods, with the most likely upper and lower intercepts for this sample at ca. 1.1 ± 0.05 Ga and 0.4 ± 0.2 Ga, respectively. There are also minor increases in likelihood for upper intercepts at ca. 2.0, 2.6, and 3.2 Ga that broadly correspond to age peaks observed in the previous samples. The most likely upper intercept obtained using this method is corroborated with a linear regression in *ISOPLOT*, which produces an upper intercept of 1071+98/−44 Ma (MSWD = 0.37; Fig. 8e). The ca. 1.9 Ga analyses are also suspected to have experienced Pb-loss. A Pb-loss line can be traced through these analyses to the discordant ca. 1.5–1.3 Ga analyses and even to the most discordant ca. 700 Ma analyses. However an upper concordia intercept of analyses along this line is poorly resolved via the method of Reimink et al. (2016). Instead, an upper intercept calculated using *ISOPLOT* yields an age of 2006 ± 77 Ma (MSWD = 11.8; Fig. 8f).

Hafnium isotope data were obtained for 17 zircons belonging to the ca. 1.0 Ga and 2.0 Ga populations, as well as those of ca. 0.7 Ga and 1.4 Ga age (Fig. 6). The two analyses of zircons of ca. 650 Ma age returned $\varepsilon_{Hf}(t)$ values of −15.0 and −14.9, similar to or slightly more evolved than many of the zircon grains from the ca. 1.0 Ga population, providing a small indication that these grains may have initially belonged to the ca. 1.0 Ga population. Zircon grains from the ca. 1.0 Ga population have $\varepsilon_{Hf}(t)$ values ranging from −25.0 to −4.4, with the exception of two grains that have $\varepsilon_{Hf}(t)$ values of +1.2 and + 3.9. A single ca. 1.3 Ga grain yielded an $\varepsilon_{Hf}(t)$ value of +5.4. Analyses from the 1.8 Ga population yielded two $\varepsilon_{Hf}(t)$ values of −2.2 and −0.5, comparable to values obtained for similar populations from the other samples analysed in this study. Trace element data (Fig. 7c) for this sample show a distinct REE enrichment for two analyses in comparison to the other obtained analyses, which is particularly noticeable in the light REE concentrations for these zircons. Such variance may reflect a difference in source material or subsequent metamorphism (Hoskin and Schaltegger, 2003; Wang et al., 2016). These zircons yielded crystallisation ages of ca. 1.02 Ga and 1.05 Ga, which is temporally indistinct from the majority of analyses from this sample. Morphologically, these zircons are largely indistinct from other grains of similar age in this sample, though are slightly darker in CL. P contents obtained for this sample range from ~150 ppm to 700 ppm (Fig. 7d).

4.2. Irumide Belt samples

Three samples from the Irumide Belt were analysed for Lu–Hf isotopic data. These samples were previously collected and analysed for U–Pb geochronology by De Waele et al. (2006a), with detailed sample descriptions provided therein.

4.2.1. Sample IL14

Sample IL14 is a quartzite sampled from the Ilondola Mission area. The U–Pb zircon data were previously reported in De Waele et al. (2006a) and display prominent age populations at ca. 1.9, 2.0–2.1, 2.2, 2.4, 2.7, 2.9 and 3.0 Ga. Forty-one analyses were undertaken on grains from this sample. $\varepsilon_{Hf}(t)$ values obtained from these analyses range from −9.8 to +6.5 (Fig. 5), with all but three analyses returning a negative $\varepsilon_{Hf}(t)$ value. Notably, the three positive analyses were obtained from the grains with oldest three U–Pb ages (ca. 3.0–2.7 Ga) obtained from this sample.

4.2.2. Sample KAS

Sample KAS is a quartzite sampled near Kasama. This sample contains zircon age populations of ca. 1.4, 1.8–1.9, 2.0, 2.1, 2.2 and 2.6 Ga (De Waele et al., 2006a). Twenty-nine analyses were obtained from this sample, with obtained $\varepsilon_{Hf}(t)$ values ranging from −6.6 to +1.7 (Fig. 5). The positive $\varepsilon_{Hf}(t)$ values obtained can be observed to from a cluster at ca. 1.87 Ga.

4.2.3. Sample MA6

Detrital zircon sample MA6 is a quartzite from near Mansa. Previously collected zircon U–Pb data indicates age populations at ca. 1.9, 2.0, 2.2, 2.4 and 2.7 Ga (De Waele et al., 2006a). Thirty-nine analyses were obtained from this sample, with $\varepsilon_{Hf}(t)$ values that range from −11.3 to +7.7 (Fig. 5). Only two analyses provide

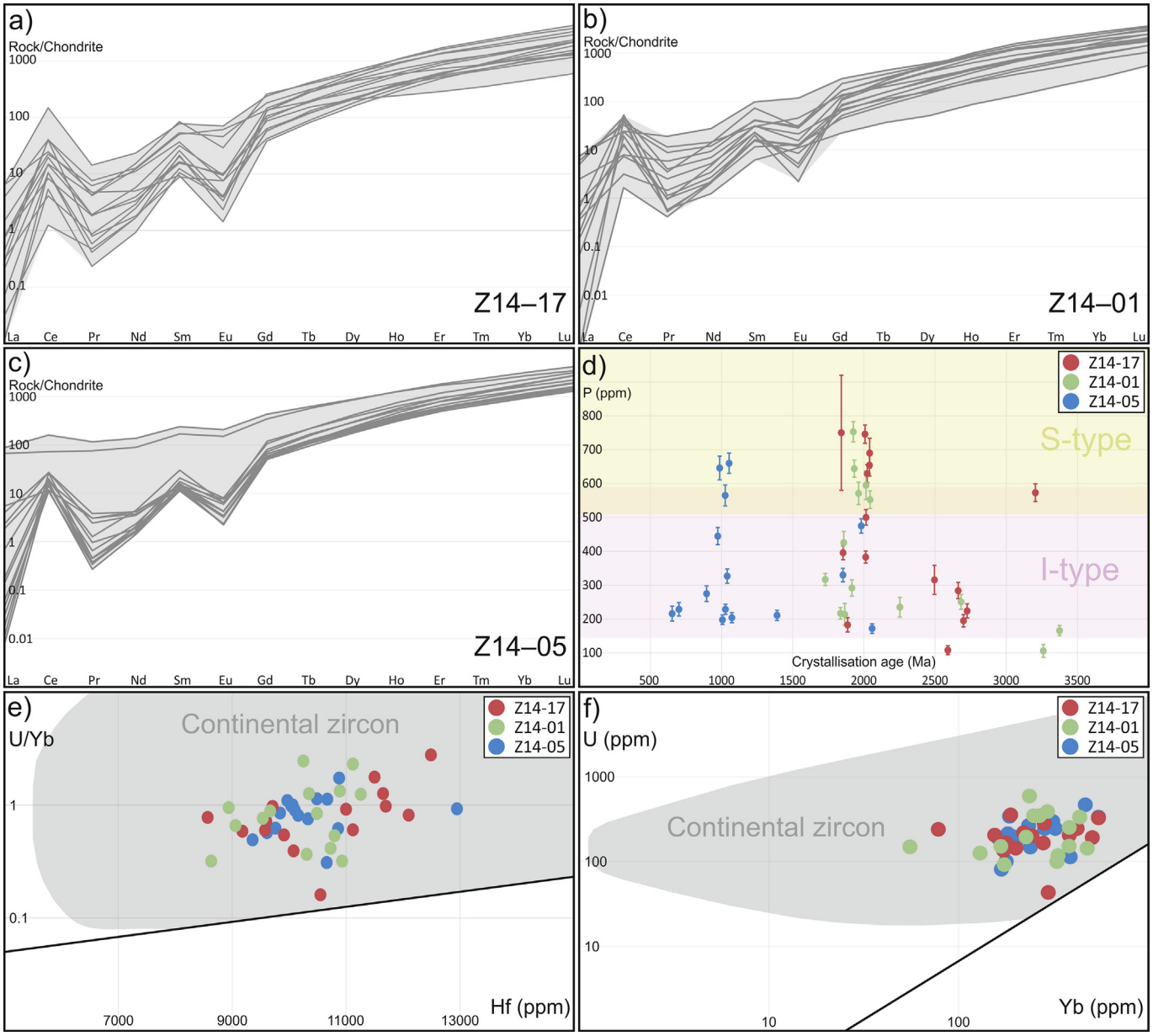

Figure 7. Trace element diagrams for samples from the SIB terranes. (a–c) Rare-earth element diagrams normalised to the average chondrite (McDonough and Sun, 1995) for samples Z14-17, Z14-01 and Z14-05, respectively; (d) Phosphorous contents versus U–Pb age diagram for Z14 samples; (e) U/Yb versus Hf diagram for Z14 samples, with the grey field outlining the values for continental zircons (Grimes et al., 2007); (f) U versus Yb diagram for Z14 samples, with the grey field outlining the values for continental zircons (Grimes et al., 2007).

positive values. The analysis returning an $\varepsilon_{Hf}(t)$ value of +7.7 was obtained from the second oldest (ca. 2.9 Ga) grain analysed for this sample.

5. Discussion

5.1. Depositional age constraints on Southern Irumide Belt protoliths

Sample Z14-17 was sourced from the western-most Chewore–Rufunsa Terrane of the SIB. From this sample the youngest age population was found to be ca. 1.8 Ga, the youngest ≤10% discordant analysis yielded a $^{207}Pb/^{206}Pb$ age of 1768.1 ± 58.4 Ma (2σ uncertainty) that is interpreted to represent the maximum depositional age of this sample. Johnson et al. (2006) described quartzite in the Chewore–Rufunsa Terrane as distributed between Mesoproterozoic volcanic and pelitic rocks. This terrane has been shown to have experienced widespread magmatism and metamorphism in the period between ca. 1095 Ma and 1040 Ma (Goscombe et al., 2000; Johnson et al., 2006, 2007b). The sample is interpreted to have been metamorphosed during this event and hence ca. 1095 Ma is taken to represent the minimum depositional age of this sample.

Samples Z14-01 and Z14-02 were sourced from the Kacholola Terrane. From these samples, the youngest population identified is ca. 1.85 Ga in age. The youngest ≤10% discordant analysis was from Z14-01 yielded a $^{207}Pb/^{206}Pb$ age of 1764.4 ± 74.2 Ma (2σ uncertainty) and is taken to represent the maximum depositional age of both samples. Igneous intrusions are rare within this terrane (Johnson et al., 2006) and there are a general lack of geochronological data that constrain the timing of metamorphism in this terrane. However, low Th/U metamorphic rims from the ca. 2.6 Ga

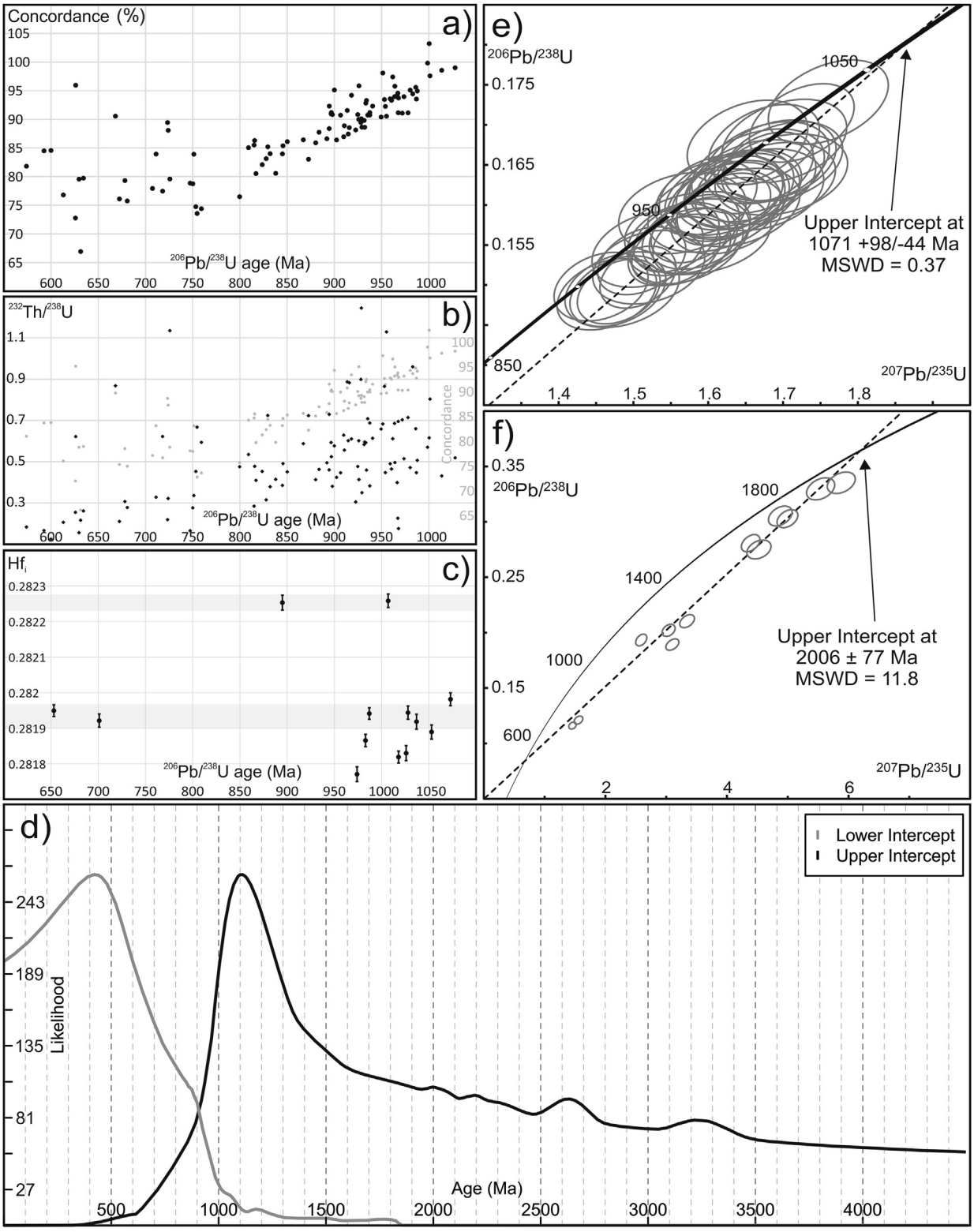

Figure 8. Plots indicating Pb-loss is recorded in zircon grains from sample Z14-05 and calculated concordia intercepts. (a) Concordance versus ^{206}Pb/^{238}U age plot; (b) ^{232}Th/^{238}U ratio versus ^{206}Pb/^{238}U age plot. Concordance versus ^{206}Pb/^{238}U age is additionally shown on the secondary vertical axis (light grey); (c) Hf$_i$ versus ^{206}Pb/^{238}U age plot; (d) Upper concordia intercept calculated for the ca. 1.0 Ga population using *ISOPLOT*; (e) Upper concordia intercept calculated for grains of a suspected ca. 2 Ga population using *ISOPLOT*; (f) most likely upper and lower concordia intercepts (ca. 1.1 Ga and 0.4 Ga, respectively) for sample Z14-05, obtained using the modelling method of Reimink et al. (2016).

basement granodiorite were dated at ca. 1.04 Ga (Cox et al., 2002). We suggest this metamorphism is contemporaneous with that observed in the overlying sedimentary rocks in this terrane, and thus, reflects the minimum depositional age for these samples.

Sample Z14-05 was collected from the Nyimba–Sinda Terrane, the youngest $^{206}Pb/^{238}U$ age (≤5% discordant) is 626.1 ± 17.2 Ma (2σ uncertainty). Depletion in ^{232}Th and a decreasing $^{232}Th/^{238}U$ ratio is typical of post-crystallisation isotope remobilization in zircon (Pidgeon, 1992; Pidgeon et al., 1998; Ashwal et al., 1999; Vavra et al., 1999; Hoskin and Black, 2000; Collins, 2003; Collins et al., 2004; Kirkland et al., 2015) and is a visible feature in the ca. 850–600 Ma zircon from sample Z14-05 (Fig. 8b). Hf stochiometrically replaces Zr in the zircon crystal structure, and is usually retained in the event of Pb loss. As such, grains that were subjected to post-crystallisation Pb loss are likely to retain their initial Hf values (Finch and Hanchar, 2003; Hawkesworth and Kemp, 2006). Zircon grains with ages that are younger than ca. 1.0 Ga have Hf_i values that are the same as those displayed in the ca. 1.0 Ga population (Fig. 8c), indicating that the zircon may have been derived from the same crystallisation event. Given the equivalent Hf_i values, decreasing $^{232}Th/^{238}U$ ratios and increasing concordance with increasing age (Fig. 8a and b), it is interpreted that these grains do not record their true age. These grains have likely undergone post-crystallisation isotope remobilization as a result of metamorphism during ca. 540 Ma collision between the Congo and Kalahari cratons. This suggests that the zircon grains may have been a part of an older (ca. 1.1–1.0 Ga) population prior to Pb loss. The obtained upper concordia intercept age of 1071 + 98/−44 Ma (MSWD = 0.37) and maximum likelihood intercept of ~1.1 Ga (Fig. 7) correspond with magmatism occurring in the SIB between ca. 1095 and 1040 Ma. The magmatism occurring at this time is suggested to represent the last source of sedimentary input to this sample and therefore, represent the maximum depositional age. We acknowledge that some of these zircon analyses may instead represent slightly younger magmatic events occurring in the Irumide Belt at ca. 1020 Ma (De Waele et al., 2006b), though resolving this conundrum is difficult with the obtained analyses. This sample of quartzite falls within the broader mapping unit of Neoproterozoic gneiss, which is widespread throughout the Nyimba–Sinda terrane. A sample of this gneiss, located ~40 km southwest of this sampling locality has a protolith age of 742 ± 13 Ma (Johnson et al., 2006). Though early work tentatively suggested that Neoproterozoic gneiss formed the basement to the overlying quartzite (Johns et al., 1989), a rigorous relationship between the gneiss and the quartzite is unclear. If the protolith to the gneiss intruded the metasediments, this would provide a direct constraint on the minimum depositional age of the sample.

5.2. Correlation and provenance of Southern Irumide Belt metasedimentary rocks

5.2.1. Chewore–Rufunsa and Kacholola terranes

Samples from the Chewore–Rufunsa (Z14-17) and Kacholola (Z14-01 and Z14-02) terranes have prominent detrital zircon U–Pb age peaks at ca. 2.0, 2.7 and 3.3 Ga, with trace element concentrations that reflect continental sources (Figs. 6f and 7e). Recently, the concentration of P in zircon has been used as a tool in distinguishing zircons derived from I- and S-type granites (Burnham and Berry, 2017). If the zircon grains from these samples were sourced from phases of predominantly granitic magmatism, grains older than ca. 2.0 Ga were likely sourced from I-type granites (Fig. 7d). Zircon grains belonging to the ca. 2.0 Ga and 1.8 Ga populations display variable P contents that could reflect I- and possibly S-type granite sources. The age populations observed in these samples correlate well with age populations reported by De Waele et al. (2006a) for the Muva Supergroup. Furthermore, the $\varepsilon_{Hf}(t)$ values obtained for Chewore–Rufunsa and Kacholola samples (Z16-17, Z16-01 and Z16-02) are identical to values obtained in this study for these same populations. Both the aforementioned terranes and Muva Supergroup display detrital zircon age peaks that correspond with the main magmatic phases observed within the Bangweulu Block (De Waele et al., 2003, 2006a, b). $\varepsilon_{Nd}(t)$ data obtained by De Waele et al. (2006b) clearly demonstrate that the igneous phases in the Bangweulu Block are the result of Proterozoic crustal reworking, which is consistent with the evolved zircons from this study. On the basis of highly correlative age populations and isotopic values, it is interpreted that the sedimentary rocks of the Chewore–Rufunsa and Kacholola terranes were derived from the same or similar source to that of the Muva Supergroup. The prominent ca. 2.0 Ga zircon grains population are likely sourced from Usagaran or Ubendian phase granites. De Waele et al. (2006b) used this term to not only encompass the magmatism occurring in the Ubendian–Usagaran Belt at this time (Ring et al., 1997; Boniface et al., 2012; Tulibonywa et al., 2015), but also in the SW Irumide Belt. As such, zircons forming the ca. 2.0 Ga age peak may have been sourced from either region. The ca. 1.8 Ga age population observed in sample Z14-17 may be derived from Usagaran or Ubendian phase intrusions, granitoids of ca. 1.85–1.80 Ga age that are speculated to have been part of a widespread plutono-volcanic province ranging from the Ubendian Belt to the Domes region of the Copperbelt in northern Zambia (De Waele et al., 2006b). The south-west Irumide Belt records ca. 2.7 Ga magmatism (De Waele, 2004; De Waele et al., 2006b) and may explain the presence of the small ca. 2.7–2.6 Ga detrital zircon age population found in samples from both terranes. Another potential source of this population can be found in the Isimani Suite of the Usagaran Belt. Here, Collins et al. (2004) reported xenocrysts of ca. 2.7 Ga age in post-tectonic granites. From these data and previous work (Maboko, 1995; Möller et al., 1995; Muhongo et al., 2001; Stern, 2002), a large volume of ca. 2.7 Ga material (subsequently reworked in the Usagaran orogen) was located to the east of the Tanzanian Craton. Three zircon grains from the three samples record ages over 3 Ga and it is possible that these are derived from a cryptic basement terrane described by De Waele et al. (2008). The proposed terrane possibly underlies both the Bangweulu Block and Irumide Belt. These authors further suggest this may be the same block that collided with the Tanzania Craton between 2 and 1.8 Ga.

The sediments of the Muva Supergroup are suggested to have correlatives in parts of both central Madagascar and Southern India (Cox et al., 2004; Plavsa et al., 2014, 2015), an interpretation made with the few data available at the time. In central Madagascar, multiple metasedimentary units preserve detrital age populations that are consistent with those observed in this study. Although the relative population sizes differ between the central Madagascan units and samples obtained in this study, the data indicate that sediments in both regions sourced similarly aged material. The Hf isotopic data obtained in this study provides a new detrital fingerprint for correlation, and indicates that the age populations common to sedimentary rocks of both the southern Congo margin and central Madagascar display broadly similar $\varepsilon_{Hf}(t)$ values. Zircons with ages between ca. 2.1 Ga and 1.9 Ga in both regions record $\varepsilon_{Hf}(t)$ values between approximately −10 and + 1. Zircons with ages between ca. 3.0 Ga and 2.5 Ga in central Madagascar record predominantly juvenile $\varepsilon_{Hf}(t)$ values, although a significant portion of samples record evolved values (Archibald et al., 2015) that are consistent with the values recorded by similarly aged grains in the Irumide and Southern Irumide belts. Few data are available for the 3.2 Ga population, although slightly evolved $\varepsilon_{Hf}(t)$ values were recorded for both regions (Archibald et al., 2015). As such, the results of this study are consistent with interpretations of the

southern and eastern margins of the Congo Craton were a source region for Archaean–Palaeoproterozoic detrital zircon found in central Madagascar. Plavsa et al. (2014) compared U–Pb and Hf isotope data from southern India to that available for the Congo Craton and central Madagascar, interpreting a correlation between units in each region that was later supported with the data obtained by Archibald et al. (2015). With the exception of the ca. 3.2 Ga population, U–Pb age populations identified in this study are similarly present in those identified in sediments from southern India. Hf data is not available for ca. 1.9 Ga zircon grains. For those belonging to older populations $\varepsilon_{Hf}(t)$ values range from approximately −5 to +10 and are predominantly juvenile (Plavsa et al., 2014). This is contrary to Hf data collected in this study, where sediments older than 2.0 Ga have evolved isotopic signatures. More data are required to thoroughly constrain the sediment sources in this region but the southern Congo margin could, at the very least, be a partial sediment source.

5.2.2. Nyimba–Sinda Terrane

Sample Z14-05 was collected from the Nyimba–Sinda Terrane, and displays age peaks at ca. 1.0 Ga and 1.9 Ga. We interpret the 1.9 Ga population to have been subjected to Pb loss, as such an upper concordia intercept of 2006 ± 77 Ma is used to characterise this peak. This age suggests that this population may have been derived from Usagaran phase granites, similar to the samples from the Chewore–Rufunsa and Kacholola terranes. Similarly, the 1.0 Ga population is interpreted to have been subjected to Pb loss. We instead argue that the upper intercepts show that the analyses formed a single coherent population at ca. 1.1–1.0 Ga (Fig. 8d and e). This age indicates that the sample and associated sedimentary sequence represent a younger cover sequence post-dating orogenesis in the region at ca. 1090–1020 Ma. Arc magmatism in the SIB has been shown to have occurred between ca. 1095 Ma and 1040 Ma (Johnson et al., 2006, 2007b; Westerhof et al., 2008) and involved the contamination of juvenile material by silicic continental crust, typical of a continental-margin-arc setting (Johnson et al., 2007b). On the basis of the age and isotopic nature of this magmatism, we suggest these intrusions provide an ideal sediment source for Z14-05. Other possible sediment sources can be found along the southern Congo margin, and further afield in Africa. Similarly aged (ca. 1.1–1 Ga) sediments can be found in southern Zambia, as part of a supracrustal sequence in the Zambezi Belt (Johnson et al., 2007a). These sediments are thought to have been deposited on the southern Congo margin, and sourced directly from underlying basement that could also represent a source for the Nyimba–Sinda sediments. Contemporaneous rocks in western Madagascar (Dabolava Suite; ca. 1080–980 Ma) were recently interpreted to represent oceanic arc relicts that were part of the same arc as the Irumide Belt at this time (Archibald et al., 2017). Juvenile $\varepsilon_{Hf}(t)$ values with only minor deflection to evolved values in conjunction with $\delta^{18}O$ data were interpreted to indicate the incorporation of young sedimentary or volcanic rocks into evolving juvenile ca. 1080–980 Ma magmas (Archibald et al., 2017). The $\varepsilon_{Hf}(t)$ values obtained in this study for similarly aged zircons are predominantly evolved, though two grains display juvenile values equivalent with those obtained by Archibald et al. (2017). As such, plutonic and volcanic rocks in western Madagascar are unlikely to be the source for these ca. 1.1–1.0 Ga detrital zircons.

5.3. Palaeogeographic implications

The geochronological data gathered in this study for sedimentary rocks of the Chewore–Rufunsa and Kacholola terranes strongly suggests that they were derived from the same sources as the Muva Supergroup. Such a correlation may indicate that–contrary to previous interpretations–the Chewore–Rufunsa and Kacholola terranes of the SIB were depositionally connected and hence, adjacent to or in close proximity to the Irumide Belt. Such implications may extend to the terranes and complexes in Mozambique and Tanzania that are suggested to be a continuation of the SIB (Westerhof et al., 2008; Bingen et al., 2009; Thomas et al., 2016). Previous interpretations contradict this hypothesis, instead arguing that the SIB collided with the southern Congo margin after forming on the Rushinga microcontinent (Fig. 9; Johnson et al., 2005, 2007; Begg et al., 2009). These alternative interpretations cite the likely presence of the Mwembeshi Shear Zone between the two belts (reactivating the suture between the belts), and their contrasting styles of metamorphism. However, rigorous pressure–temperature estimates are not available for most regions in either belt, and recent estimates obtained for the Chipata Terrane instead appear to indicate that both the Irumide and Southern Irumide belts experienced similar pressures of metamorphism during the same period (Karmakar and Schenk, 2016), which may contradict the basis for these interpretations. As such, it remains a plausible scenario that at least the Zambian terranes of the SIB originally formed on the Congo margin and were available for sedimentation from Muva Supergroup sources, similar to sequences in the Irumide Belt (Fig. 10). This suggests that the Palaeoproterozoic basement of the SIB is the same basement to that of the Irumide Belt, and implies the SIB did not form on a discrete micro-continental mass that later collided with the southern Congo margin. The Luangwa Valley (and possibly Mwembeshi Shear Zone) located between the Irumide and Southern Irumide belts may instead reflect the site of thinned continental crust that experienced multiple periods of extension and contraction. We suggest an alternative model where the gap in magmatic ages recorded in the southern Irumide Belt (ca. 1095–1040 Ma) and Irumide Belt (ca. 1020 Ma) reflects the magmatic front migrating towards the foreland in response to a shallowing subduction zone. Such a feature is documented in the Andes (Fig. 9; Ramos and Folguera, 2005), with a spatial and temporal gap (~100 km and 40 Ma) in magmatic fronts that is similar to that recorded in the Irumide and Southern Irumide belts. If rifting subsequently separated a micro-continental mass from the southern Congo margin (forming the Rushinga Microcontinent), it would be equivalent to basement located on the southern Congo Craton. The plausibility of these interpretations are dependent on the remaining work to be done to constrain the relationship between the Irumide and Southern Irumide belts.

Detrital zircons from Z14-05 indicate that this sample is part of a cover sequence present within the Nyimba–Sinda terrane that post-dates the orogenic events occurring in the SIB and Irumide Belts between ca. 1095 Ma and 1020 Ma (Johnson et al., 2007b). The extent of this cover sequence is unknown, though it appears to correlate with sedimentary rocks in northeast Mozambique and southern Tanzania, which yield similar age populations and depositional constraints to the analysed sample (Fig. 10; Bingen et al., 2009; Thomas et al., 2016). This sequence likely includes the extensive carbonates preserved in the Nyimba–Sinda Terrane, with marbles similarly preserved in southern Tanzania. The prominent ca. 1.0 Ga age peak and isotopic nature of zircons from Z14-05 are consistent with SIB magmatism and possibly crustal melting in the Irumide Belt. Widespread Neoproterozoic gneiss occurs within this terrane, in close association with the potentially rift related volcanic rocks (Barr and Drysdall, 1972; Johnson et al., 2006). This led Johnson et al. (2006) to speculate that this terrane could represent rifting between the Congo and Kalahari cratons. Similarly aged (714 ± 17 Ma) magmatism has been identified in northeast Mozambique (Bjerkgard et al., 2009), which is also interpreted as part of a continental rift related cover sequence (Bingen et al., 2009). If these sequences do indeed have a rift related origin,

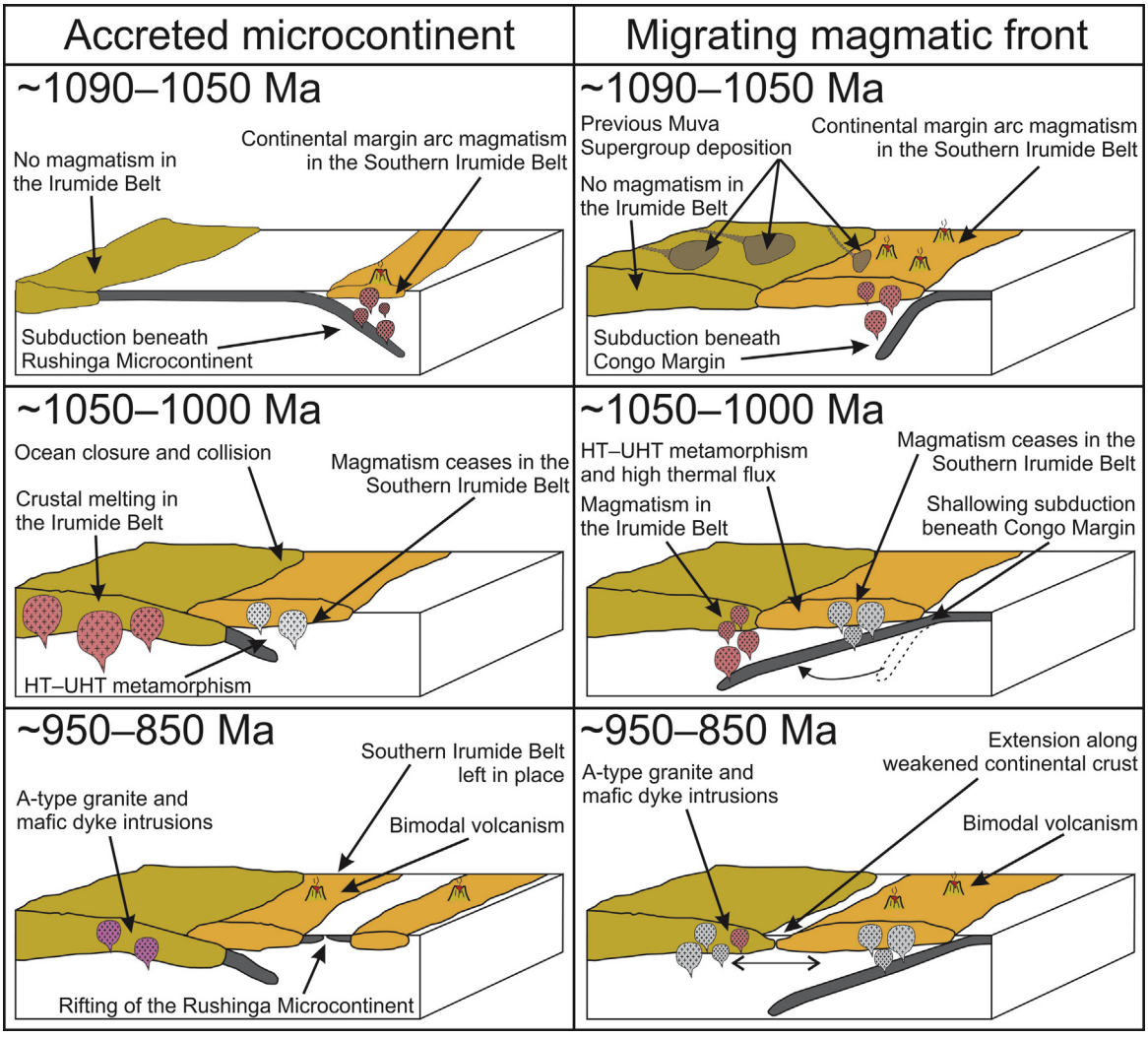

Figure 9. Simplified diagram of the tectonic development of the Irumide and Southern Irumide belts along the southern margin of the Congo Craton from ca. 1100 Ma to 850 Ma. The left column displays the sequences of events along the southern Congo margin hypothesised by a model where the SIB formed on a microcontinent that subsequently collided with the Irumide Belt (De Waele et al., 2006b; Karmakar and Schenk, 2016). The right column displays the sequence of events hypothesised by a model where the SIB initially formed along the southern Congo margin, and evolved in a similar fashion to the Andes (Ramos and Folguera, 2005).

then the timing of their formation supports the Neoproterozoic model of Merdith et al. (2017). These authors interpret such rifting along the southern margin of the Congo Craton at this time, occurring as an extension of the spreading system that served to separate the Australian Plate from Laurentia during the initial breakup of Rodinia (Fig. 10).

6. Conclusions

Detrital zircons in metasedimentary rocks of the Chewore–Rufunsa and Kacholola terranes are Palaeoarchaean to Palaeoproterozoic in age and are derived from relatively evolved sources, reflecting the reworking of crustal material. These sedimentary protoliths were deposited between ca. 1.8 Ga and 1.1 Ga. Similar age peaks and isotopic characteristics of zircon grains from these western terranes of the SIB suggest that they correlate with the Muva Supergroup (or at least share the same sources). Whether the sedimentary protoliths reflect these terranes forming on the edge of the Congo Craton, or instead reflect the deposition of sediments from the same sources on to an advancing Rushinga microcontinent that collided with the Congo Craton, remains unresolved. Further east in the SIB, detrital zircons in metasedimentary rocks of the Nyimba–Sinda Terrane show a marked difference in age, ranging from Palaeoproterozoic to Neoproterozoic. The sedimentary protoliths here were deposited between ca. 900 Ma and 740 Ma, suggesting that this is a Neoproterozoic cover sequence with correlatives elsewhere within the SIB, in northeast Mozambique and southern Tanzania. Detrital zircons of this terrane display U–Pb ages and $\varepsilon_{Hf}(t)$ values that suggest that they are sourced from ca. 1095–1040 Ma continental-margin-arc magmatism in the SIB and possibly ca. 1020 Ma crustal anatexis in the Irumide Belt. Age and depositional constraints indicate that these sedimentary protoliths were deposited after magmatism and metamorphism in the Irumide and Southern Irumide belts. We suggest that this cover sequences, and its correlatives in Mozambique and Tanzania, reflect a history of Neoproterozoic extension that is intermittently recorded throughout the SIB. Such extension is interpreted to reflect rifting occurring on the southern margin of the Congo Craton during initial break up of Rodinia. This study serves to highlight the enigmatic development of much of the SIB, and its relationship to the Irumide Belt. Additional work is required to rigorously constrain the evolution of this region to

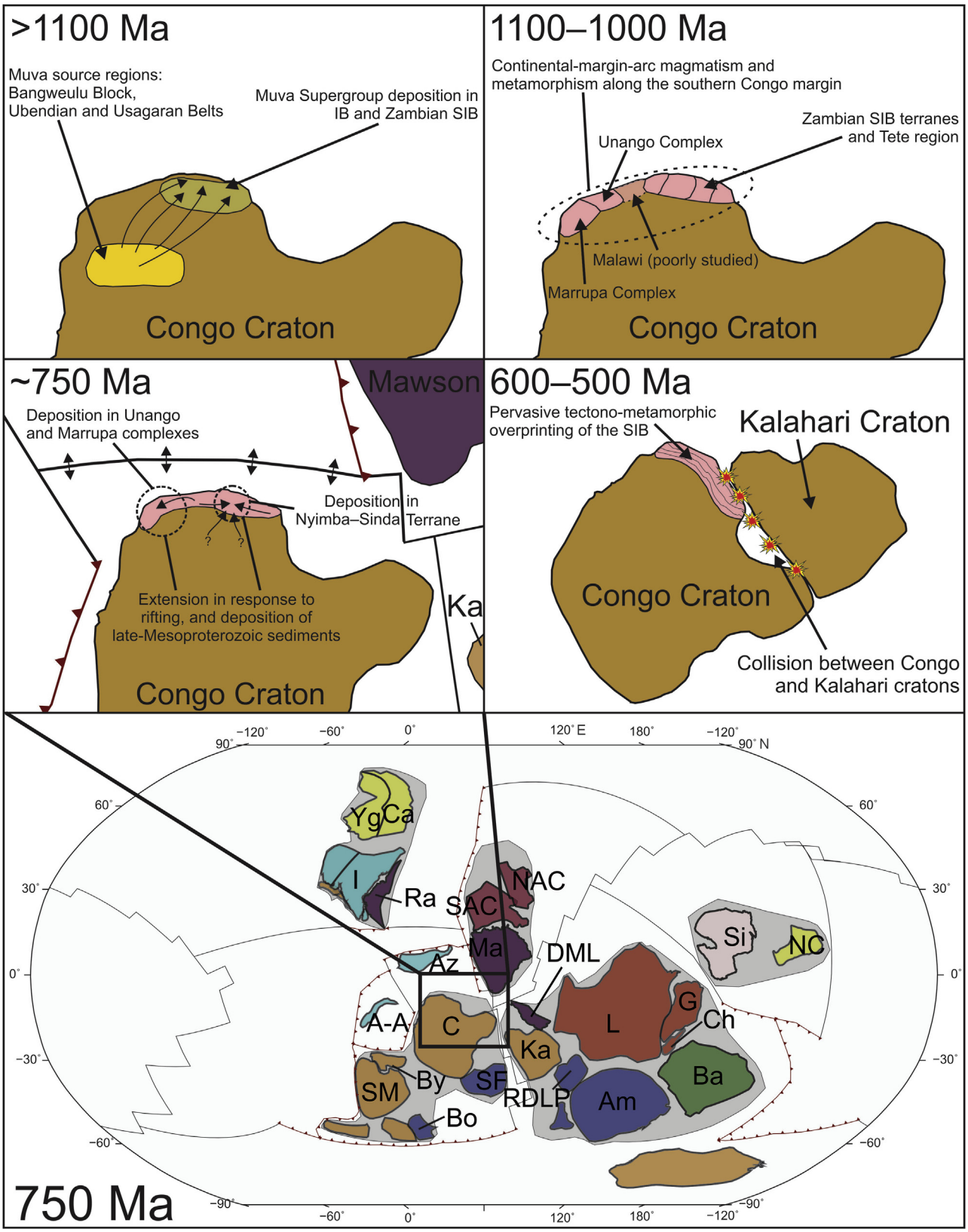

Figure 10. Series of palaeogeographic cartoons showing the interpreted development of the southern Congo margin from ca. 1100 to 500 Ma. The cartoons depict interpreted sequences of deposition, magmatism, and metamorphism in the SIB, culminating with pervasive overprinting as a result of the collision between the Congo and Kalahari cratons in the later stages of Gondwana amalgamation. The ca. 750 Ma cartoon is linked to a palaeogeographic reconstruction for the Earth at this time, adapted from Merdith et al. (2017). Yg, Yangtze; Ca, Cathaysia; NC, North China; I, India; Az, Azania; A-A, Afif–Abas; NAC, North Australian Craton; SAC, South Australian Craton; Ma, Mawson; DML, Dronning Maud Land; L, Laurentia; G, Greenland; Ch, Chortis; SM, Sahara Metacraton; By, Bayuda; C, Congo; Ka, Kalahari; Bo, Borborema; SF, São Francisco; RDLP, Rio de la Plata; Am, Amazonia; Ba, Baltica; Si, Siberia.

determine the tectonic implications for the development of the southern Congo Craton and central Gondwana during the Neoproterozoic.

Acknowledgements

This paper forms TRaX record #402 and is a contribution to IGCP projects #628 (Gondwana Map) and #648 (Supercontinents and Global Dynamics). This project was funded by Australian Research Council Future Fellowship #FT120100340 to A. Collins. B. Wade, S. Gilbert and A. McFadden of Adelaide Microscopy are thanked for their help with collection of analytical data. B. Alessio is supported by a Research Training Program scholarship. Comments from R. Thomas greatly improved this contribution.

References

Agar, R., 1984. Geological Map of the Petauke Area. Geol. Survey Zambia. Government of the United Kingdom (Ordnance Survey).

Archibald, D.B., Collins, A.S., Foden, J.D., Payne, J.L., Macey, P.H., Holden, P., Razakamanana, T., 2017. Stenian–Tonian arc magmatism in west–central Madagascar: the genesis of the Dabolava Suite. Journal of the Geological Society jgs2017–jgs2028. https://doi.org/10.1144/jgs2017-028.

Archibald, D.B., Collins, A.S., Foden, J.D., Payne, J.L., Taylor, R., Holden, P., Razakamanana, T., Clark, C., 2015. Towards unravelling the Mozambique Ocean conundrum using a triumvirate of zircon isotopic proxies on the Ambatolampy Group, central Madagascar. Tectonophysics 662, 167–182.

Ashwal, L.D., Tucker, R.D., Zinner, E.K., 1999. Slow cooling of deep crustal granulites and Pb-loss in zircon. Geochimica et Cosmochimica Acta 63, 2839–2851.

Barr, M., Drysdall, A., 1972. The Geology of the Sasare Area: Explanation of Degree Sheet 1331, SW Quarter. Government Printer, South Africa.

Begg, G., Griffin, W., Natapov, L., O'Reilly, S.Y., Grand, S., O'Neill, C., Hronsky, J., Djomani, Y.P., Swain, C., Deen, T., 2009. The lithospheric architecture of Africa: seismic tomography, mantle petrology, and tectonic evolution. Geosphere 5, 23–50.

Bingen, B., Jacobs, J., Viola, G., Henderson, I., Skår, Ø., Boyd, R., Thomas, R., Solli, A., Key, R., Daudi, E., 2009. Geochronology of the Precambrian crust in the Mozambique belt in NE Mozambique, and implications for Gondwana assembly. Precambrian Research 170, 231–255.

Bjerkgard, T., Stein, H., Bingen, B., Henderson, I., Sandstad, J., Moniz, A., 2009. The Niassa Gold Belt, northern Mozambique–A segment of a continental-scale Pan-African gold-bearing structure? Journal of African Earth Sciences 53, 45–58.

Boniface, N., Schenk, V., Appel, P., 2012. Paleoproterozoic eclogites of MORB-type chemistry and three Proterozoic orogenic cycles in the Ubendian Belt (Tanzania): evidence from monazite and zircon geochronology, and geochemistry. Precambrian Research 192, 16–33.

Boyd, R., Nordgulen, Ø., Thomas, R., Bingen, B., Bjerkgård, T., Grenne, T., Henderson, I., Melezhik, V., Often, M., Sandstad, J., 2010. The geology and geochemistry of the East African Orogen in northeastern Mozambique. South African Journal of Geology 113, 87–129.

Brewer, M., Haslam, H., Darbyshire, P., Davis, A., 1979. Rb-sr Age Determinations in the Bangweulu Block, Luapula Province. Zambia Institute of Geological Sciences, London, 79/5.

Burnham, A., Berry, A., 2017. Formation of Hadean granites by melting of igneous crust. Nature Geoscience 10, 457–461.

Collins, A.S., 2003. Structure and age of the northern Leeuwin Complex, Western Australia: constraints from field mapping and U–Pb isotopic analysis. Australian Journal of Earth Sciences 50, 585–599.

Collins, A.S., Pisarevsky, S.A., 2005. Amalgamating eastern Gondwana: the evolution of the circum-indian orogens. Earth-Science Reviews 71, 229–270.

Collins, A.S., Reddy, S.M., Buchan, C., Mruma, A., 2004. Temporal constraints on Palaeoproterozoic eclogite formation and exhumation (Usagaran Orogen, Tanzania). Earth and Planetary Science Letters 224, 175–192.

Collins, A.S., Windley, B.F., 2002. The tectonic evolution of central and northern Madagascar and its place in the final assembly of Gondwana. The Journal of Geology 110, 325–339.

Corfu, F., Hanchar, J.M., Hoskin, P.W., Kinny, P., 2003. Atlas of zircon textures. Reviews in Mineralogy and Geochemistry 53, 469–500.

Cox, R., Armstrong, R.A., Ashwal, L.D., 1998. Sedimentology, geochronology and provenance of the Proterozoic Itremo Group, central Madagascar, and implications for pre-Gondwana palaeogeography. Journal of the Geological Society 155, 1009–1024.

Cox, R., Coleman, D.S., Chokel, C.B., DeOreo, S.B., Wooden, J.L., Collins, A.S., De Waele, B., Kröner, A., 2004. Proterozoic tectonostratigraphy and paleogeography of Central Madagascar derived from detrital zircon U-Pb age populations. The Journal of Geology 112, 379–399.

Cox, R., Rivers, T., Mapani, B., Tembo, D., De Waele, B., 2002. New U-Pb data for the irumide belt: LAM-ICP-MS results for Luangwa terrane. In: 11th IAGOD Quadrennial Symposium and Geocongress, p. 10. Technical Meeting IGCP.

Daly, M., 1986. The intracratonic Irumide belt of Zambia and its bearing on collision orogeny during the Proterozoic of Africa. Geological Society, London, Special Publications 19, 321–328.

Daly, M., Chakraborty, S., Kasolo, P., Musiwa, M., Mumba, P., Naidu, B., Namateba, C., Ngambi, O., Coward, M., 1984. The Lufilian arc and Irumide belt of Zambia: results of a geotraverse across their intersection. Journal of African Earth Sciences (1983) 2, 311–318.

Daly, M., Unrug, R., 1982. The Muva Supergroup of Northern Zambia: A Craton to Mobile Belt Sedimentary Sequence, vol. 85. Verhandelinge van die Geologiese Vereniging van Suid-Afrika, pp. 155–165.

De Waele, B., 2004. The Proterozoic Geological History of the Irumide Belt, Zambia.

De Waele, B., Fitzsimons, I., 2007. The nature and timing of Palaeoproterozoic sedimentation at the southeastern margin of the Congo Craton; zircon U–Pb geochronology of plutonic, volcanic and clastic units in northern Zambia. Precambrian Research 159, 95–116.

De Waele, B., Fitzsimons, I., Wingate, M., Tembo, F., Mapani, B., Belousova, E., 2009. The geochronological framework of the Irumide Belt: a prolonged crustal history along the margin of the Bangweulu Craton. American Journal of Science 309, 132–187.

De Waele, B., Johnson, S.P., Pisarevsky, S.A., 2008. Palaeoproterozoic to Neoproterozoic growth and evolution of the eastern Congo Craton: its role in the Rodinia puzzle. Precambrian Research 160, 127–141.

De Waele, B., Kampunzu, A.B., Mapani, B.S.E., Tembo, F., 2006a. The mesoproterozoic irumide belt of Zambia. Journal of African Earth Sciences 46, 36–70.

De Waele, B., Liégeois, J.-P., Nemchin, A.A., Tembo, F., 2006b. Isotopic and geochemical evidence of proterozoic episodic crustal reworking within the irumide belt of south-central Africa, the southern metacratonic boundary of an Archaean Bangweulu Craton. Precambrian Research 148, 225–256.

De Waele, B., Mapani, B., 2002. Geology and correlation of the central Irumide belt. Journal of African Earth Sciences 35, 385–397.

De Waele, B., Wingate, M.T., Fitzsimons, I.C., Mapani, B.S., 2003. Untying the Kibaran knot: a reassessment of Mesoproterozoic correlations in southern Africa based on SHRIMP U-Pb data from the Irumide belt. Geology 31, 509–512.

Dhuime, B., Hawkesworth, C., Cawood, P., 2011. When continents formed. Science 331, 154–155.

Finch, R.J., Hanchar, J.M., 2003. Structure and chemistry of zircon and zircon-group minerals. Reviews in Mineralogy and Geochemistry 53, 1–25.

Fitzsimons, I., Hulscher, B., Collins, A., 2004. Structural, metamorphic and SHRIMP U–Pb age data from the Pan-African of Madagascar: evidence for multi-stage assembly of the East African Orogen. 20th Colloquium of African Geology, BRGM, Orleans, France, p. 164.

Goscombe, B., Armstrong, R., Barton, J., 2000. Geology of the Chewore inliers, Zimbabwe: constraining the mesoproterozoic to palaeozoic evolution of the Zambezi belt. Journal of African Earth Sciences 30, 589–627.

Griffin, W., Wang, X., Jackson, S., Pearson, N., O'Reilly, S.Y., Xu, X., Zhou, X., 2002. Zircon chemistry and magma mixing, SE China: in-situ analysis of Hf isotopes, Tonglu and Pingtan igneous complexes. Lithos 61, 237–269.

Grimes, C.B., John, B.E., Kelemen, P., Mazdab, F., Wooden, J., Cheadle, M.J., Hanghøj, K., Schwartz, J., 2007. Trace element chemistry of zircons from oceanic crust: a method for distinguishing detrital zircon provenance. Geology 35, 643–646.

Hanson, R., 2003. Proterozoic geochronology and tectonic evolution of southern Africa. Geological Society, London, Special Publications 206, 427–463.

Hauzenberger, C., Tenczer, V., Bauernhofer, A., Fritz, H., Klötzli, U., Košler, J., Wallbrecher, E., Muhongo, S., 2014. Termination of the southern irumide belt in Tanzania: zircon U/Pb geochronology. Precambrian Research 255, 144–162.

Hawkesworth, C., Kemp, A., 2006. Using hafnium and oxygen isotopes in zircons to unravel the record of crustal evolution. Chemical Geology 226, 144–162.

Hoskin, P., Black, L., 2000. Metamorphic zircon formation by solid-state recrystallization of protolith igneous zircon. Journal of Metamorphic Geology 18, 423–439.

Hoskin, P.W., Ireland, T.R., 2000. Rare earth element chemistry of zircon and its use as a provenance indicator. Geology 28, 627–630.

Hoskin, P.W., Schaltegger, U., 2003. The composition of zircon and igneous and metamorphic petrogenesis. Reviews in Mineralogy and Geochemistry 53, 27–62.

Jackson, S.E., Pearson, N.J., Griffin, W.L., Belousova, E.A., 2004. The application of laser ablation-inductively coupled plasma-mass spectrometry to in situ U–Pb zircon geochronology. Chemical Geology 211, 47–69.

Johns, C.C., Liyungu, K., Mabuku, S., Mwale, G., Sakungo, F., Tembo, D., Vallance, G., Barr, M.W.C., 1989. The stratigraphic and structural framework of Eastern Zambia: results of a geotraverse. Journal of African Earth Sciences (and the Middle East) 9, 123–136.

Johnson, S., De Waele, B., Evans, D., Banda, W., Tembo, F., Milton, J., Tani, K., 2007a. Geochronology of the Zambezi Supracrustal sequence, southern Zambia: a record of Neoproterozoic divergent processes along the southern margin of the Congo Craton. The Journal of Geology 115, 355–374.

Johnson, S., De Waele, B., Liyungu, A., 2006. U-Pb SHRIMP geochronology of granitoid rocks in eastern Zambia: terrane subdivision of the Mesoproterozoic Southern Irumide Belt. Tectonics 25.

Johnson, S.P., De Waele, B., Tembo, F., Katongo, C., Tani, K., Chang, Q., Iizuka, T., Dunkley, D., 2007b. Geochemistry, geochronology and isotopic evolution of the chewore–rufunsa terrane, southern irumide belt: a mesoproterozoic continental margin arc. Journal of Petrology 48, 1411–1441.

Johnson, S.P., Rivers, T., De Waele, B., 2005. A review of the Mesoproterozoic to early Palaeozoic magmatic and tectonothermal history of south–central Africa: implications for Rodinia and Gondwana. Journal of the Geological Society 162, 433–450.
Karmakar, S., Schenk, V., 2016. Mesoproterozoic UHT metamorphism in the southern irumide belt, Chipata, Zambia: petrology and in situ monazite dating. Precambrian Research 275, 332–356.
Kirkland, C., Smithies, R., Taylor, R., Evans, N., McDonald, B., 2015. Zircon Th/U ratios in magmatic environs. Lithos 212, 397–414.
Kröner, A., Cordani, U., 2003. African, southern Indian and South American cratons were not part of the Rodinia supercontinent: evidence from field relationships and geochronology. Tectonophysics 375, 325–352.
Ludwig, K., 2004. Users Manual for ISOPLOT/EX, Version3. 1. A Geochronological Toolkit for Microsoft Excel, vol. 4. Berkeley Geochronology Center, Special Publication.
Maboko, M., 1995. Neodymium isotopic constraints on the protolith ages of rocks involved in Pan-African tectonism in the Mozambique Belt of Tanzania. Journal of the Geological Society 152, 911–916.
Macey, P.H., Thomas, R.J., Grantham, G.H., Ingram, B.A., Jacobs, J., Armstrong, R.A., Roberts, M.P., Bingen, B., Hollick, L., de Kock, G.S., Viola, G., Bauer, W., Gonzales, E., Bjerkgård, T., Henderson, I.H.C., Sandstad, J.S., Cronwright, M.S., Harley, S., Solli, A., Nordgulen, Ø., Motuza, G., Daudi, E., Manhiça, V., 2010. Mesoproterozoic geology of the Nampula block, northern Mozambique: tracing fragments of mesoproterozoic crust in the heart of Gondwana. Precambrian Research 182, 124–148.
Mapani, B., Rivers, T., Tembo, F., De Waele, B., Katongo, C., 2004. Growth of the Irumide terranes and slices of Archaean age in eastern Zambia. Geoscience Africa 2004, 414–415. Abstract 2.
Mapani, B., Rivers, T., Tembo, F., Katongo, C., 2001. Terrane mapping in the eastern Irumide and Mozambique belts: implications for the assembly and dispersal of Rodinia. In: IGCP, pp. 10–11.
McDonough, W.F., Sun, S.-S., 1995. The composition of the Earth. Chemical Geology 120, 223–253.
McGee, B., Halverson, G.P., Collins, A.S., 2012. Cryogenian rift-related magmatism and sedimentation: south-western Congo Craton, Namibia. Journal of African Earth Sciences 76, 34–49.
Merdith, A.S., Collins, A.S., Williams, S.E., Pisarevsky, S., Foden, J.F., Archibald, D., Blades, M.L., Alessio, B.L., Armistead, S., Plavsa, D., 2017. A full-plate global reconstruction of the Neoproterozoic. Gondwana Research 50, 84–134.
Möller, A., Appel, P., Mezger, K., Schenk, V., 1995. Evidence for a 2 Ga subduction zone: eclogites in the Usagaran belt of Tanzania. Geology 23, 1067–1070.
Muhongo, S., Kröner, A., Nemchin, A., 2001. Single zircon evaporation and SHRIMP ages for granulite-facies rocks in the Mozambique belt of Tanzania. The Journal of Geology 109, 171–189.
Oliver, G., Johnson, S., Williams, I., Herd, D., 1998. Relict 1.4 Ga oceanic crust in the Zambezi Valley, northern Zimbabwe: evidence for Mesoproterozoic supercontinental fragmentation. Geology 26, 571–573.
Paton, C., Hellstrom, J., Paul, B., Woodhead, J., Hergt, J., 2011. Iolite: freeware for the visualisation and processing of mass spectrometric data. Journal of Analytical Atomic Spectrometry 26, 2508–2518.
Payne, J.L., Pearson, N.J., Grant, K.J., Halverson, G.P., 2013. Reassessment of relative oxide formation rates and molecular interferences on in situ lutetium–hafnium analysis with laser ablation MC-ICP-MS. Journal of Analytical Atomic Spectrometry 28, 1068–1079.
Pidgeon, R., 1992. Recrystallisation of oscillatory zoned zircon: some geochronological and petrological implications. Contributions to Mineralogy and Petrology 110, 463–472.
Pidgeon, R., Nemchin, A., Hitchen, G., 1998. Internal structures of zircons from Archaean granites from the Darling Range batholith: implications for zircon stability and the interpretation of zircon U-Pb ages. Contributions to Mineralogy and Petrology 132, 288–299.
Plavsa, D., Collins, A.S., Foden, J.D., Clark, C., 2015. The evolution of a Gondwanan collisional orogen: a structural and geochronological appraisal from the Southern Granulite Terrane, South India. Tectonics 34, 820–857.
Plavsa, D., Collins, A.S., Payne, J.L., Foden, J.D., Clark, C., Santosh, M., 2014. Detrital zircons in basement metasedimentary protoliths unveil the origins of southern India. The Geological Society of America Bulletin 126, 791–811.
Ramos, V.A., Folguera, A., 2005. Tectonic evolution of the Andes of Neuquén: constraints derived from the magmatic arc and foreland deformation. Geological Society, London, Special Publications 252, 15–35.
Ray, A., 1984. Geological Map of the Rufunsa Area. Geol. Survey Zambia. Government of the United Kingdom (Ordnance Survey).
Reimink, J.R., Davies, J.H., Waldron, J.W., Rojas, X., 2016. Dealing with discordance: a novel approach for analysing U–Pb detrital zircon datasets. Journal of the Geological Society 2015–2114.
Ring, U., Kröner, A., Toulkeridis, T., 1997. Palaeoproterozoic granulite-facies metamorphism and granitoid intrusions in the Ubendian-Usagaran Orogen of northern Malawi, east-central Africa. Precambrian Research 85, 27–51.
Sarafian, E., Evans, R.L., Abdelsalam, M.G., Atekwana, E., Elsenbeck, J., Jones, A.G., Chikambwe, E., 2018. Imaging Precambrian lithospheric structure in Zambia using electromagnetic methods. Gondwana Research 54, 38–49.
Schandelmeier, H., 1980. Regionale Gliederung des Präkambriums und Aspekte der Krustenentwicklungum Mambwe, Nordost-Zambia. Lenz.
Schandelmeier, H., 1983. The geochronology of post-Ubendian granitoids and dolerites from the Mambwe area, northern province, Zambia. Report of the Institute of Geological Sciences 83, 40–46.
Sláma, J., Košler, J., Condon, D.J., Crowley, J.L., Gerdes, A., Hanchar, J.M., Horstwood, M.S., Morris, G.A., Nasdala, L., Norberg, N., 2008. Plešovice zircon—a new natural reference material for U–Pb and Hf isotopic microanalysis. Chemical Geology 249, 1–35.
Stern, R.J., 2002. Crustal evolution in the East African Orogen: a neodymium isotopic perspective. Journal of African Earth Sciences 34, 109–117.
Thomas, R.J., Bushi, A.M., Roberts, N.M., Jacobs, J., 2014. Geochronology of granitic rocks from the Ruangwa region, southern Tanzania–Links with NE Mozambique and beyond. Journal of African Earth Sciences 100, 70–80.
Thomas, R.J., Spencer, C., Bushi, A.M., Baglow, N., Boniface, N., de Kock, G., Horstwood, M.S., Hollick, L., Jacobs, J., Kajara, S., 2016. Geochronology of the central Tanzania Craton and its southern and eastern orogenic margins. Precambrian Research 277, 47–67.
Tulibonywa, T., Manya, S., Maboko, M.A., 2015. Palaeoproterozoic volcanism and granitic magmatism in the Ngualla area of the Ubendian Belt, SW Tanzania: constraints from SHRIMP U–Pb zircon ages, and Sm–Nd isotope systematics. Precambrian Research 256, 120–130.
Vavra, G., Schmid, R., Gebauer, D., 1999. Internal morphology, habit and U-Th-Pb microanalysis of amphibolite-to-granulite facies zircons: geochronology of the Ivrea Zone (Southern Alps). Contributions to Mineralogy and Petrology 134, 380–404.
Vayrda, I., 1984. Geological Map of the Chipata Area. Geol. Survey Zambia. Government of the United Kingdom (Ordnance Survey).
Wang, C., Liang, X., Foster, D.A., Fu, J., Jiang, Y., Dong, C., Zhou, Y., Wen, S., Van Quynh, P., 2016. Detrital zircon U–Pb geochronology, Lu–Hf isotopes and REE geochemistry constrains on the provenance and tectonic setting of Indochina Block in the Paleozoic. Tectonophysics 677, 125–134.
Westerhof, A.P., Lehtonen, M.I., Mäkitie, H., Manninen, T., Pekkala, Y., Gustafsson, B., Tahon, A., 2008. The Tete-Chipata Belt: a new multiple terrane element from western Mozambique and southern Zambia. Geological Survey of Finland Special Paper 48, 145–166.
Woodhead, J., Hergt, J., Shelley, M., Eggins, S., Kemp, R., 2004. Zircon Hf-isotope analysis with an excimer laser, depth profiling, ablation of complex geometries, and concomitant age estimation. Chemical Geology 209, 121–135.